

A Velocity-Entropy Invariance theorem for the Chapman-Jouguet detonation

Pierre Vidal* and Ratiba Zitoun†

Institut Pprime, UPR 3346 CNRS, ENSMA, BP40109, 86961 Futuroscope-Chasseneuil, FRANCE

(Dated: May 6, 2022 - Update of the 1st version, June 20, 2020, arXiv:2006.12533)

The velocity and the specific entropy of the Chapman-Jouguet (CJ) equilibrium detonation in a homogeneous explosive are shown to be invariant under the same variations of the initial pressure and temperature. The CJ state, including the adiabatic exponent, and its isentrope, can then be obtained from the CJ velocity or, conversely, the CJ velocity from one CJ variable, without equation of state of detonation products. For gaseous explosives, comparison to calculations with detailed chemical equilibrium shows agreement to within $\mathcal{O}(0.1)\%$. However, the CJ pressures of four carbonate liquid explosives are found about 20 % greater than measured values: the CJ-equilibrium model appears not to apply to carbonate condensed explosives. A simple criterion for assessing the representativeness of this model is thus proposed, which nevertheless cannot indicate which of its assumptions would not be satisfied, such as chemical equilibrium or single-phase fluid. This invariance might be an illustration of a general feature of hyperbolic systems and their characteristic surfaces.

I. INTRODUCTION

The Chapman-Jouguet (CJ) detonation [1] is a classic of combustion theory defined as the fully-reactive, planar, and compressive discontinuity wave, with a constant velocity supersonic with respect to the initial state, and sonic with respect to the final burnt state at chemical equilibrium. The CJ state and velocity thus derive from the Rankine-Hugoniot relations and the equation of state of detonation products. Although their representativeness is now accepted as uncertain because detonation dynamics is unstable and very sensitive to losses, the CJ model remains the staple of detonation theory to easily obtain reference velocities and reaction-end states: they are a predictable limit independently of any condition for detonation existence. It is the purpose of this study to bring out and investigate two supplemental CJ properties [2] perhaps useful to help interpret experiments and improve modelling.

The first one is that the CJ detonation velocity D_{CJ} and the specific entropy s_{CJ} of a homogeneous explosive substance are invariant under the same variations of the initial temperature T_0 and pressure p_0 : if one is invariant, so is the other; different initial states producing the same D_{CJ} produce different CJ states on the same isentrope. The second one is that a CJ state and its isentrope can then be easily calculated from the value of D_{CJ} without equilibrium equation of state; conversely, D_{CJ} can be obtained from one CJ variable. These results apply only to explosives whose fresh and burnt states obey thermodynamic relationships for single-phase inviscid fluids, with temperature T and pressure p as independent variables. Figure 1 depicts the CJ model and the Velocity-Entropy invariance (DSI) theorem in the Pressure (p) - Volume (v) plane based on usual properties of detonation modelling (Sect. II).

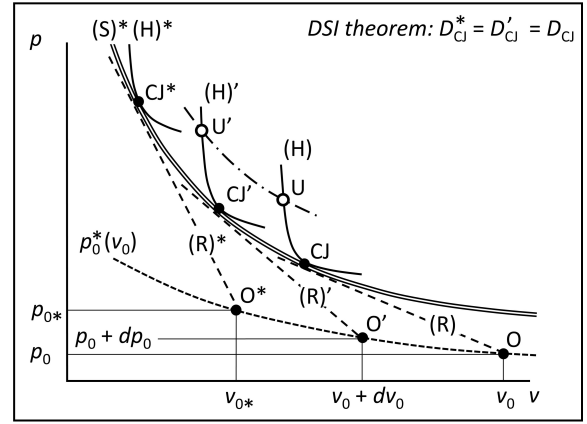


FIG. 1. An equilibrium isentrope of detonation products (S)* can be the common envelope of equilibrium Hugoniot curves (H)*, (H)' and (H) and Rayleigh-Michelson lines (R)*, (R)' and (R) if their poles O*, O' and O lie on a specific $p_0^*(v_0)$ line through a reference initial state O*(p_{0*}, v_{0*}) (the Hugoniot curvatures are accentuated). The slopes $-(D_{CJ}/v_0)^2$ of these (R) lines increase with increasing initial volume v_0 , but the DSI theorem ensures they have the same CJ velocity D_{CJ}^* . This determines the CJ*, CJ' and CJ states, the $p_0^*(v_0)$ initial states, and the isentrope (S)*, given D_{CJ}^* and the initial sound speeds and Gruneisen coefficients.

Is the detonation regime identifiable from experimental detonation velocities and pressures? Models are generally rejected if they cannot represent the observations, but their assumptions may not be physically relevant to the experiments, differences may be due to imprecise measurements or non-physical parameters, and an agreement should not exclude fewer assumptions. Equations of state of detonation products are calibrated by fitting the calculated CJ properties to the experimental values, although no criteria ensure the latter are those of the CJ-equilibrium detonation. This study proposes they are not if they do not satisfy the supplemental properties.

* pierre.vidal@cnrs.pprime.fr, @ensma.fr

† ratiba.zitoun@univ-poitiers.fr, @ensma.fr

Efforts today focus less on the physical relevance of the CJ model than on the identification and the modelling of processes in the reaction zones of detonations such as losses, adiabatic or not, non-local thermodynamics, cellular instabilities in homogeneous explosives, carbon condensation or local heat exchanges between grains in heterogeneous explosives. Most of these processes can prevent reaching the CJ-equilibrium state. Its usefulness is essentially to be an ideal thermodynamic limit for calibrating the equations of state of detonation products, whether or not the reactive flow reaches chemical equilibrium.

To some degree, this work also extends the semiempirical Inverse Method of Jones [3], Stanyukovich [4] and Manson [5]. The Inverse Method gives the CJ hydrodynamic variables from experimental values of D_{CJ} and its derivatives with respect to two independent initial-state variables, such as p_0 and T_0 (Subsect. III.D, §2); this work shows that the only value of D_{CJ} is sufficient.

Section II is a reminder on classical but necessary elements that also introduces the main notation, Section III sets out the DSI theorem and the CJ supplemental properties, Section IV is an analysis of their agreements or differences with calculations or measurements for gases and liquids, and Section V is a summary with some speculative conclusions.

II. REMINDERS AND NOTATION

The CJ postulate is that the sonic and equilibrium constraints are satisfied at the same position in the flow. This is in fact more of an ideal mathematical limit than observable physical reality. The traditional introduction to this old issue is the Zel'dovich-von Neuman-Döring (ZND) detonation model, that is, a leading shock sustained by a subsonic laminar reaction zone [6]. A self-sustained detonation is such that the sonic front of the rear expansion maintains a sufficient distance from the shock so the progress of the chemical process is large enough, depending on the interplay between flow dynamics and physicochemical processes. The ZND model uses the frozen sound speed, the CJ model uses the equilibrium sound speed.

A. Where the Chapman-Jouguet model lies

Most explosive devices have finite transverse dimensions, so self-sustained detonations are non-ideal, with diverging reaction zones that encompass a frozen sonic locus, hence curved leading shocks and velocities smaller than the planar CJ one: the flow behind the sonic locus cannot sustain the shock. However, not any reaction process can reach CJ equilibrium as the steady planar limit of a sonic curved detonation [7]. A presentation of equilibrium-frozen issues and several non-ideal detonations was given by Higgins [8]. At the sonic locus,

the rates of reaction processes, possibly non-monotonic, exothermic or endothermic [9, 10], have to offset those of losses, such as heat transfer, friction or transverse expansion of the reaction zone, so that the flow derivatives remain finite there. The dynamics of a self-sustained detonation is thus described by an Eigen-constraint between the parameters of the reaction and loss rates [11] and those of the leading-shock, namely its normal velocity, acceleration and curvature [12–15]. Achieving the CJ balance at least requires set-ups large enough that losses are negligible and the detonation front is flat, and distances from the ignition position long enough that the gradients of the expanding flow of products are small, so the chemical equilibrium can shift continuously.

Reaction processes differ for gases and liquids. For gases, up to moderately large equivalence ratios (ER), the prevailing view is that the translation, rotation and vibration degrees of freedom re-equilibrate much faster than chemical kinetics. For liquids, molecular-bond breaking would make the deexcitation time of vibrations comparable to that of chemical relaxation [16]. An introduction to the Non-Equilibrium ZND model was given by Tarver [17]. Local thermodynamic equilibrium would be reached before chemical transformation in such gases but perhaps not in the detonation products of liquids. For gases with very large ERs, several works, e.g. [18–21], point out that solid carbon condensation decrease the detonation velocity with increasing ERs faster than predicted by calculations that model the detonation products as a homogeneous gas. Carbon condensation is also likely inherent to detonation in many condensed explosives, as most are over-carbonated [22–24]. The DSI theorem is restricted to detonation products described as a single-phase fluid at chemical equilibrium.

The main criticism of the ZND model for homogeneous explosives is the instability of their reaction zones: they are not laminar, and detonation fronts have a three-dimensional structure. In gases, the flow advects unburnt pockets, the front has a cellular structure, and the experimental mean widths of detonation cells are 10 to 50 times greater than calculated characteristic thicknesses of planar steady ZND reaction zones [25, 26], even if such widths can be difficult to define. In liquids, instabilities have often been observed, but their relation to chemical kinetics and their similarities to those in gases are still being investigated [24, 27–30]. The surface areas of the detonation front or the cross-section of the experimental device at least have to be large enough compared to the mean width of the instabilities for the CJ properties can be representative averages.

The CJ supplemental properties in this work do not aim at indicating which of the CJ assumptions is not satisfied, namely sonic chemical equilibrium, single-phase fluid, or laminar flow. However, they provide a simple criterion for determining whether the CJ-equilibrium model can represent experimental and numerical data because they do not necessitate specifying the equation of state.

B. Thermodynamic and hydrodynamic relations

Single-phase inviscid fluids, whether inert or at chemical equilibrium, have two independent state variables, namely temperature T and pressure p , but specific volume $v(T, p)$ is more convenient than T for hydrodynamics because it appears explicitly in the balance equations. Specific enthalpy h and entropy s are the main state functions used in this work; their differentials write

$$dh(s, p) = Tds + vdp, \quad (1)$$

$$dh(p, v) = \frac{G+1}{G}vdp + \frac{c^2}{G}\frac{dv}{v}, \quad (2)$$

$$dh(T, p) = C_p dT + \left(1 - \frac{T}{v} \frac{\partial v}{\partial T}\right)_p vdp, \quad (3)$$

$$Tds(p, v) = \frac{vdp}{G} + \frac{c^2}{G}\frac{dv}{v}, \quad (4)$$

$$c^2 = Gv \left(\frac{\partial h}{\partial v}\right)_p = -v^2 \left(\frac{\partial p}{\partial v}\right)_s, \quad (5)$$

$$G = \frac{v}{\left(\frac{\partial h}{\partial p}\right)_v - v} = -\frac{v}{T} \left(\frac{\partial T}{\partial v}\right)_s, \quad (6)$$

where c is the sound speed, G is the Gruneisen coefficient and C_p is the heat capacity at constant pressure. In gases, the adiabatic exponent γ defines the convenient representation of c

$$c^2 = \gamma pv, \quad \gamma = -\frac{v}{p} \left(\frac{\partial p}{\partial v}\right)_s. \quad (7)$$

In the p - v plane, isentropes ($ds = 0$) have negative slopes since $\gamma > 0$, and their local convexities are defined by the sign of the fundamental derivative of hydrodynamics Γ [31–34] (most fluids have uniformly convex isentropes: $\Gamma > 0$, their slopes monotonically decrease with increasing volume),

$$\Gamma = \frac{1}{2} \frac{v^3}{c^2} \frac{\partial^2 p}{\partial v^2} \bigg|_s = \frac{-v}{2} \frac{\partial^2 p}{\partial v^2} \bigg|_s / \left(\frac{\partial p}{\partial v}\right)_s = 1 - \frac{v}{c} \frac{\partial c}{\partial v} \bigg|_s. \quad (8)$$

The fresh (initial, subscript 0) and the equilibrium (final, no subscript) states of a reactive medium have different state functions and coefficients because their chemical compositions are different. Typically, $\gamma < \gamma_0$ and, if products are brought from a (T, p) equilibrium state to the (T_0, p_0) initial state, $v(T_0, p_0) > v_0 = v_0(T_0, p_0)$ and $h(T_0, p_0) < h_0 = h_0(T_0, p_0)$. The difference of enthalpies $Q_0 = h_0(T_0, p_0) - h(T_0, p_0)$ at (T_0, p_0) is the heat of reaction at constant pressure.

Conservation of mass, momentum and energy surface fluxes through hydrodynamic discontinuities is expressed by the Rankine-Hugoniot relations, which, along the nor-

mal to the discontinuity, write

$$\rho_0 D = \rho(D - u), \quad (9)$$

$$p_0 + \rho_0 D^2 = p + \rho(D - u)^2, \quad (10)$$

$$h_0 + \frac{1}{2}D^2 = h + \frac{1}{2}(D - u)^2, \quad (11)$$

where $\rho = 1/v$ is the specific mass, and u and D are the material speed and the discontinuity velocity in a laboratory-fixed frame, with initial state at rest ($u_0 = 0$). These relations combined with an $h(p, v)$ equation of state are not a closed system since there are 4 equations for the 5 variables v, p, h, u and D , given an initial state (p_0, v_0) and $h_0(p_0, v_0)$, hence a one-variable solution, for example

$$p, v, h, u, T, s, c, \gamma, \Gamma, G, \dots \equiv \eta(D; v_0, p_0). \quad (12)$$

Its representation in the p - v plane (Fig. 2) is an intersect of a Rayleigh-Michelson (R) line $p_R(v, D; v_0, p_0)$ and the Hugoniot (H) curve $p_H(v; v_0, p_0)$,

$$p_R: \quad p = p_0 + \left(\frac{D}{v_0}\right)^2 (v_0 - v), \quad (13)$$

$$p_H: \quad h(p, v) = h_0(p_0, v_0) + \frac{1}{2}(p - p_0)(v_0 + v). \quad (14)$$

A Hugoniot for a detonation ($Q_0 > 0$, $v(T_0, p_0) > v_0$) lies above that for a shock ($Q_0 = 0$, $v(T_0, p_0) = v_0$): most fluids have uniformly-convex Hugoniots with 1 compressive intersect (N, $v/v_0 < 1$) if $Q_0 = 0$ regardless of D , and 2 (U and L) if $Q_0 > 0$ and D is large enough (Fig. 2). The observability of states on non-uniformly-convex Hugoniots is an open debate on whether theoretical instability criteria are met in Nature, based on linear and non-linear stability analyses of discontinuities [35–39]. At least physical admissibility (the discontinuity increases entropy, $s > s_0$) or equivalently mathematical determinacy (uniqueness and continuous dependency of (12) on the flow boundaries) have to be satisfied [40–42]. Denoting by M_0 and M the discontinuity Mach numbers relative to the initial and the final states, this is expressed by the subsonic-supersonic evolution condition

$$u + c > D > c_0 \Leftrightarrow \frac{D}{c_0} = M_0 > 1 > M = \frac{D - u}{c}. \quad (15)$$

C. Chapman-Jouguet states and velocities, and a remark

The tangency of a Rayleigh-Michelson line $p_R(v; D)$, an equilibrium Hugoniot $p_H(v)$ and an isentrope $p_S(v)$ defines CJ points and is equivalent to the sonic condition (20) below, as shown by

$$\left(\frac{\partial p_R}{\partial v}\right)_{D,p_0,v_0} = -\left(\frac{D}{v_0}\right)^2 < 0, \quad (16)$$

$$\left(\frac{\partial p_S}{\partial v}\right)_s = -\left(\frac{D}{v_0}\right)^2 \times M^{-2} < 0, \quad (17)$$

$$\left(\frac{\partial p_H}{\partial v}\right)_{p_0,v_0} = -\left(\frac{D}{v_0}\right)^2 \times \left(1 + 2\frac{M^{-2} - 1}{F}\right), \quad (18)$$

$$F(G, v; v_0) = 2 - G\left(\frac{v_0}{v} - 1\right), \quad (19)$$

$$M_{CJ} = \left(\frac{D - u}{c}\right)_{CJ} = 1 \text{ or } D_{CJ} = (u + c)_{CJ}. \quad (20)$$

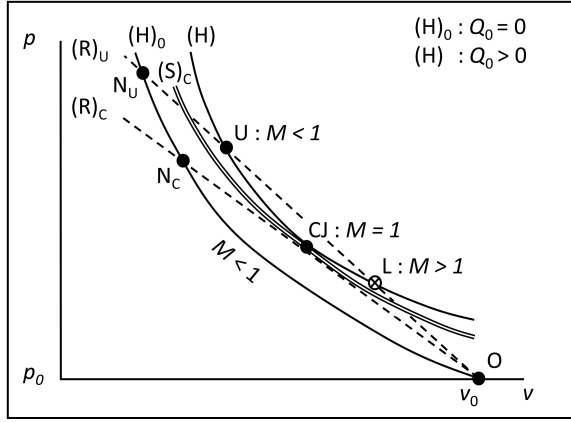


FIG. 2. Unreacted $(H)_0$ and equilibrium (H) Hugoniot curves, and Rayleigh-Michelson (R) lines, $(R)_U$ and $(R)_C$, for discontinuity velocities greater than or equal to D_{CJ} . Physical intersects are points N , U and CJ ($M \leq 1 \leq M_0$), the CJ isentrope $(S)_C$ is positioned between the $(R)_C$ line and the (H) curve.

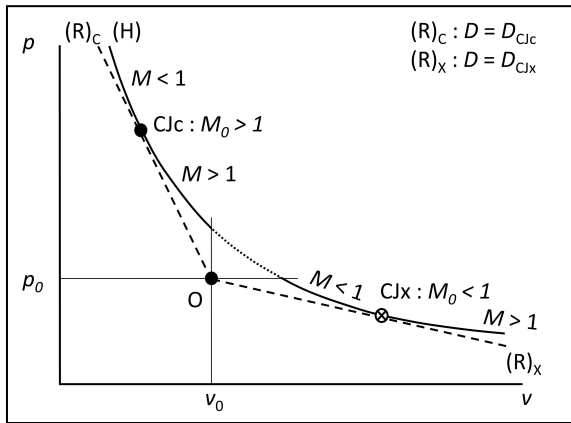


FIG. 3. Detonation (upper) and deflagration (lower) Hugoniot arcs; the physical branch is above the compressive CJ point CJ_c .

There are at least 2 CJ points, such as on uniformly-convex Hugoniot (Fig. 3). The upper, compressive, one

(CJ_c) is the CJ detonation, with minimum velocity supersonic with respect to the initial state ($v_{CJ}/v_0 < 1$, $p_{CJ}/p_0 > 1$, $D_{CJc}/c_0 > 1$). The lower, expansive, one (CJ_x) is the CJ deflagration, with maximum velocity subsonic with respect to the initial state ($v_{CJ}/v_0 > 1$, $p_{CJ}/p_0 < 1$, $D_{CJx}/c_0 < 1$).

The admissibility of the CJ detonation requires $\Gamma_{CJ} > 0$ (App. B), which implies that $F > 0$ about and at a CJ point, that the physical branch of an equilibrium Hugoniot arc is convex and above the CJ point as M decreases from 1 and s increases with decreasing v , and that $p_S(v)$ is positioned between $p_H(v)$ and $p_R(v)$ if $G > 0$. The other properties useful here are $0 \leq \partial s_H / \partial D)_{p_0, v_0} < \infty$ regardless of M , and, since $F_{CJ} \neq 0$, $\partial s_H / \partial v)_{p_0, v_0}^{CJ} = 0$ and $\partial D / \partial v)_{p_0, v_0}^{CJ} = 0$, as shown by

$$\left(\frac{v_0 T}{D^2} \frac{\partial s_R}{\partial v}\right)_{D, p_0, v_0} = \frac{v}{v_0} \frac{M^{-2} - 1}{G}, \quad (21)$$

$$\left(\frac{v_0 T}{D^2} \frac{\partial s_H}{\partial v}\right)_{p_0, v_0} = -\left(1 - \frac{v}{v_0}\right) \frac{M^{-2} - 1}{F}, \quad (22)$$

$$\left(\frac{T}{D} \frac{\partial s_H}{\partial D}\right)_{p_0, v_0} = \left(1 - \frac{v}{v_0}\right)^2 > 0, \quad (23)$$

$$\left(\frac{v_0}{D} \frac{\partial D}{\partial v}\right)_{p_0, v_0} = -\left(1 - \frac{v}{v_0}\right)^{-1} \frac{M^{-2} - 1}{F}. \quad (24)$$

The CJ condition (20) closes system (2), (9)-(11): the one-variable solution (12) and (20) give the CJ velocities D_{CJ} and variables $\eta_{CJ} = (p, v, h, u, T, s, c, \gamma, \Gamma, G, \dots)_{CJ}$ as functions of the initial state,

$$D_{CJ} = D_{CJ}(v_0, p_0), \quad \eta_{CJ} = \eta_{CJ}(v_0, p_0). \quad (25)$$

Explicit solutions can be obtained with simple $h(p, v)$ equations of state (App. A). In practice, CJ detonation properties are calculated through thermochemical codes implementing physical equilibrium equations of state and thermodynamic properties at high pressures and temperatures.

The hydrodynamic variables $z = (p, v, u, c)$ at CJ points have a well-known two-variable representation as functions of D_{CJ} and γ_{CJ}

$$z_{CJ} = z_{CJ}(D_{CJ}, \gamma_{CJ}; v_0, p_0), \quad (26)$$

that is, D_{CJ} can be expressed as a function of two CJ variables, for example $D_{CJ}(v_{CJ}, \gamma_{CJ}; v_0, p_0)$: the mass balance (9) and the (R) relation (13) combined with (7) and the CJ condition (20) thus give

$$\frac{v_{CJ}}{v_0} = \frac{c_{CJ}}{D_{CJ}} = \frac{\gamma_{CJ}}{\gamma_{CJ} + 1} \left(1 + \frac{p_0 v_0}{D_{CJ}^2}\right), \quad (27)$$

$$\frac{v_0 p_{CJ}}{D_{CJ}^2} = \frac{1 + \frac{p_0 v_0}{D_{CJ}^2}}{\gamma_{CJ} + 1}, \quad (28)$$

$$\frac{u_{CJ}}{D_{CJ}} = \frac{1 - \gamma_{CJ} \frac{p_0 v_0}{D_{CJ}^2}}{\gamma_{CJ} + 1}; \quad (29)$$

the Hugoniot relation (14) then gives h_{CJ} . Thus, it can be observed that the zero-variable representation (25) is obtained from a complete set that includes the energy balance and an explicit equation of state, hence the two-variable representation (26) since it does not use these 2 relations: γ_{CJ} is simply a substitute to c_{CJ} . The DSI theorem (Sect. III) supplements (26) by including the energy balance: its primary consequence is that z_{CJ} and γ_{CJ} are explicit one-variable functions of D_{CJ} (Subsect. III-D),

$$z_{\text{CJ}} = z_{\text{CJ}}(D_{\text{CJ}}; v_0, p_0), \quad \gamma_{\text{CJ}} = \gamma_{\text{CJ}}(D_{\text{CJ}}; v_0, p_0). \quad (30)$$

Conversely, D_{CJ} is a function of one CJ variable, for example $D_{\text{CJ}}(\gamma_{\text{CJ}}; v_0, p_0)$. The NASA computer program CEA [43] for calculating chemical equilibria in ideal gases is used in subsection IV-A for investigating the theorem and generating CJ properties for comparison to the theoretical ones (30).

III. THE INVARIANCE THEOREM

Considering different initial states of the same homogeneous explosive, equivalent statements are:

1. the CJ velocity D_{CJ} and specific entropy s_{CJ} are invariant under the same initial variations;
2. CJ detonations with the same D_{CJ} have the same s_{CJ} , and conversely;
3. different initial states chosen that D_{CJ} is invariant determine different CJ states that lie on the same isentrope;
4. an isentrope is the common envelope of Hugoniot curves and Rayleigh-Michelson lines of CJ detonations with the same velocity;
5. the variations of D_{CJ} and s_{CJ} are proportional to each other, so

$$dD_{\text{CJ}} = 0 \Leftrightarrow ds_{\text{CJ}} = 0 \quad \text{or} \quad D_{\text{CJ}} = D_{\text{CJ}}(s_{\text{CJ}}). \quad (31)$$

The CJ state is the solution to the system of compatibility constraints on these initial variations. The subsections below detail the initial-variations problem, the Rankine-Hugoniot differentials, the theorem demonstration and its geometrical interpretation (Fig. 1), and the CJ supplemental properties.

A. The initial-variations problem

The simplest flow behind a planar discontinuity propagating on a constant initial state (v_0, p_0) is ahead of a piston with a constant speed u_p . The flow is constant-state and subsonic, regardless of u_p behind a shock with the same initial and final compositions, but only if u_p is greater than the CJ material speed u_{CJ} (29)

behind a detonation with final state at chemical equilibrium. This defines the constant-velocity overdriven detonation. Its velocity D and final-state variables $\eta = (p, v, h, T, s, c, \gamma, \Gamma, G, \dots)$, with $u = u_p$, are then one-variable functions (Subsect. 3.2), such as $D(u; v_0, p_0)$ and $\eta(u; v_0, p_0)$, or, equivalently, $\eta(D; v_0, p_0)$ (12), for example (A8) and (A9).

If u_p is smaller than u_{CJ} , the flow is expanding and supersonic, but sonic just at the front: the CJ-equilibrium condition is a consequence of the Taylor-Zel'dovich-Döring (TZD) simple-wave solution $\eta(x/t)$ to the homentropic flow (uniform s) behind this constant-velocity planar front: $u + c = x/t \Rightarrow (u + c)_{\text{CJ}} = x_{\text{CJ}}/t \equiv D_{\text{CJ}}$, with t the time and x the position in the flow [11, 44, 45]. In contrast to a subsonic discontinuity ($u + c > D$), no perturbation in the flow reaches the front: $x < x_{\text{CJ}} \Rightarrow x/t = u + c < x_{\text{CJ}}/t = (u + c)_{\text{CJ}} = D_{\text{CJ}}$. This defines the CJ self sustained detonation (Subsect. 2.3), (App. B). The CJ velocity and state are then the functions $D_{\text{CJ}}(v_0, p_0)$ and $\eta_{\text{CJ}}(v_0, p_0)$ (25) of the only initial state, for example (27)-(29) and (A3).

If u_p is exactly set to u_{CJ} , the flow is both constant-state and CJ sonic: $u + c = x/t = (u + c)_{\text{CJ}} = x_{\text{CJ}}/t = D_{\text{CJ}}$. The velocity D is still equal to $D_{\text{CJ}}(v_0, p_0)$, which, therefore, is also the smallest value reachable in a series of experiments, each carried out with constant values of u_p greater than, but closer and closer to $u_{\text{CJ}}(v_0, p_0)$ from one experiment to the other. This is also the limiting flow after an infinite run distance of a CJ detonation from ignition at a fixed wall ($u_p = 0$): the slopes of the $\eta(x/t)$ profiles tend to zero as t tends to infinity at fixed position x .

An overdriven detonation can thus have the same velocity D with different initial states (v_0, p_0) if u_p is set to the necessary value greater than $u_{\text{CJ}}(v_0, p_0)$ ensuring $D(u_p; v_0, p_0) = \text{const}$. There is no reason then why one of the final-state variables should also be invariant. For the CJ sonic detonation, the same initial states turn out to ensure both D_{CJ} and the CJ specific entropy s_{CJ} are constant: their respective invariances are equivalent constraints. Specific entropy s enters the problem only through the differentials of $h(s, p)$ (1) and $s(p, v)$ (4): this initial-variations problem has to be formulated as $ds = 0$ and $dD = 0$, which entails differentiating the Rankine-Hugoniot relations (9)-(11).

B. Rankine-Hugoniot differentials

The differentials of the Rayleigh-Michelson line (13), the Hugoniot relation (14) and the $h(p, v)$ equation of state (2) form the 3×3 non-homogeneous linear system for dv , dp and dh

$$\frac{v_0 dp}{D^2} + \frac{dv}{v_0} = \dots$$

$$\dots 2 \left(1 - \frac{v}{v_0}\right) \frac{dD}{D} + \frac{v_0 dp_0}{D^2} - \left(1 - 2 \frac{v}{v_0}\right) \frac{dv_0}{v_0}, \quad (32)$$

$$2 \frac{dh}{D^2} - \left(1 + \frac{v}{v_0}\right) \frac{v_0 dp}{D^2} - \left(1 - \frac{v}{v_0}\right) \frac{dv}{v_0} = \dots$$

$$\dots - \left(1 + \frac{v}{v_0}\right) \frac{v_0 dp_0}{D^2} + \left(1 - \frac{v}{v_0}\right) \frac{dv_0}{v_0} + 2 \frac{dh_0}{D^2}, \quad (33)$$

$$\frac{dh}{D^2} - \frac{G+1}{G} \frac{v}{v_0} \frac{v_0 dp}{D^2} - \frac{M^{-2}}{G} \frac{v}{v_0} \frac{dv}{v_0} = 0, \quad (34)$$

which thus write as linear combinations of dD , dv_0 , dp_0 and dh_0 (p_0, v_0), for example,

$$(M^{-2} - 1) \frac{dv}{v_0} = - \left(1 - \frac{v}{v_0}\right) F \frac{dD}{D} \dots$$

$$\dots + \left(1 - F \frac{v}{v_0}\right) \frac{dv_0}{v_0} - \frac{1 + (1 - F) \frac{v}{v_0}}{1 - \frac{v}{v_0}} \frac{v_0 dp_0}{D^2} \dots$$

$$\dots + \frac{2 - F}{1 - \frac{v}{v_0}} \frac{dh_0}{D^2}, \quad (35)$$

$$(M^{-2} - 1) \frac{v_0 dp}{D^2} = \left(1 - \frac{v}{v_0}\right) (F + 2(M^{-2} - 1)) \frac{dD}{D} \dots$$

$$\dots - \left(1 - F \frac{v}{v_0} + (M^{-2} - 1) \left(1 - 2 \frac{v}{v_0}\right)\right) \frac{dv_0}{v_0} \dots$$

$$\dots + \frac{1 + (1 - F) \frac{v}{v_0} + (M^{-2} - 1) \left(1 - \frac{v}{v_0}\right)}{1 - \frac{v}{v_0}} \frac{v_0 dp_0}{D^2} \dots$$

$$\dots - \frac{2 - F}{1 - \frac{v}{v_0}} \frac{dh_0}{D^2}. \quad (36)$$

The differential ds of the specific entropy,

$$\frac{T ds}{D^2} = \left(1 - \frac{v}{v_0}\right)^2 \frac{dD}{D} \dots$$

$$\dots + \left(1 - \frac{v}{v_0}\right) \frac{v}{v_0} \frac{dv_0}{v_0} - \frac{v}{v_0} \frac{v_0 dp_0}{D^2} + \frac{dh_0}{D^2}, \quad (37)$$

is obtained by substituting $dh(s, p)$ (1) for dh in (33) and by eliminating $v_0 dp/D^2 + dv/v_0$ with (32). The coefficients in (35) and (36) involve the three state functions v , $F(G, v)$ (19) and M : $dh(p, v)$ introduces the two state functions G and $c = (v/v_0)(D/M)$, from (9) and (15), and v , p and h are one-variable functions, from (12). In contrast, $dh(s, p)$ does not involve c , M and F , so neither does ds .

The determinant of system (32)-(34) is $M^{-2} - 1$, and the right-hand sides of (35) and (36) have to be set to zero for CJ discontinuities ($M = 1$) so dv and dp can be finite. This defines the CJ velocity and entropy differen-

tials dD_{CJ} and ds_{CJ} , from (37), as the Eigen-constraints

$$F_{CJ} \frac{dD_{CJ}}{D_{CJ}} = \dots$$

$$\dots \frac{1 - 2 \frac{v_{CJ}}{v_0} + G_{CJ} \left(1 - \frac{v_{CJ}}{v_0} + \frac{v_0}{v_{CJ}} \frac{M_{0CJ}^{-2}}{G_0}\right)}{1 - \frac{v_{CJ}}{v_0}} \frac{dv_0}{v_0} \dots$$

$$\dots - \frac{1 - G_{CJ} \frac{v_0}{v_{CJ}} \left(1 - \frac{v_{CJ}}{v_0} + \frac{1}{G_0}\right)}{1 - \frac{v_{CJ}}{v_0}} \frac{v_0 dp_0}{D_{CJ}^2}, \quad (38)$$

$$F_{CJ} \frac{T_{CJ} ds_{CJ}}{D_{CJ}^2} = \dots$$

$$\dots \left(1 - \frac{v_{CJ}}{v_0} + \frac{2M_{0CJ}^{-2}}{G_0}\right) \frac{dv_0}{v_0} \dots$$

$$\dots + \left(1 - \frac{v_{CJ}}{v_0} + \frac{2}{G_0}\right) \frac{v_0 dp_0}{D_{CJ}^2}, \quad (39)$$

by substituting $dh_0(p_0, v_0)$ for dh_0 . They can be directly obtained from (32), (33) and $dh(s, p)$, instead of $dh(p, v)$, by using the CJ condition $M = 1$ as $c/v = D/v_0$ (9) in $ds(p, v)$ (4) and then eliminating the combination $(v_0 dp_{CJ}/D_{CJ}^2) + (dv_{CJ}/v_0) = G_{CJ}(v_0/v_{CJ})(T_{CJ} ds_{CJ}/D_{CJ}^2)$ [5, 46]. The derivation above provides the intermediate differentials (35) and (36) necessary to demonstrate the DSI theorem. Differentials (38) and (39) show that $F_{CJ} \neq 0$ (19) is also a continuity condition: small initial variations have to produce small variations of D_{CJ} and s_{CJ} (Subsect. II-B, App. B). In the acoustic limit ($D \rightarrow c_0$, $v/v_0 \rightarrow 1$, $F \rightarrow 2$), (37) and (39) coherently reduce to $dh_0(s_0, p_0)$.

The theorem demonstration is easier using a simpler writing of these differentials that introduces a distribution of p_0 and v_0 on an arbitrary polar curve $p_0^*(v_0)$ through a reference point $v_{0*}, p_{0*} = p_0^*(v_{0*})$. The initial enthalpy $h_0(p_0, v_0)$ reduces to the function $h_0^*(v_0) = h_0(p_0^*(v_0), v_0)$ of v_0 , hence, from (2),

$$\frac{v_0}{D^2} \frac{dh_0^*}{dv_0} = \frac{G_0 + 1}{G_0} \left(\frac{v_0}{D}\right)^2 \frac{dp_0^*}{dv_0} + \frac{M_0^{-2}}{G_0}. \quad (40)$$

The final-state expressions $\eta(D; v_0, p_0)$ (12) reduce to functions $\eta^*(D, v_0) = \eta(D; v_0, p_0^*(v_0))$ of D and v_0 , hence, from (35) and (37),

$$(M^{-2} - 1) \frac{dv^*}{v_0} = -F \left(1 - \frac{v}{v_0}\right) \frac{dD}{D} + \Phi_v^* \frac{dv_0}{v_0}, \quad (41)$$

$$\frac{T ds^*}{D^2} = \left(1 - \frac{v}{v_0}\right)^2 \frac{dD}{D} + \Phi_s^* \frac{dv_0}{v_0}, \quad (42)$$

where

$$\Phi_v^* = 1 - 2 \frac{v}{v_0} + G \frac{v_0}{v} \times \left\{ \left(1 - \frac{v}{v_0}\right) \frac{v}{v_0} + \frac{M_0^{-2}}{G_0} \dots \right.$$

$$\dots - \left. \left(1 - G \frac{v_0}{v} \left(1 - \frac{v}{v_0} + \frac{1}{G_0}\right)\right) \right\} \times \left(\frac{v_0}{D}\right)^2 \frac{dp_0^*}{dv_0}, \quad (43)$$

$$\Phi_s^* = \left(\left(1 - \frac{v}{v_0} \right) \frac{v}{v_0} + \frac{M_0^{-2}}{G_0} \right) \dots \\ \dots + \left(1 - \frac{v}{v_0} + \frac{1}{G_0} \right) \left(\frac{v_0}{D} \right)^2 \frac{dp_0^*}{dv_0}, \quad (44)$$

Similarly to $h_0(p_0, v_0)$, the CJ velocity $D_{\text{CJ}}(v_0, p_0)$ and specific entropy $s_{\text{CJ}}(v_0, p_0)$ reduce to the functions $D_{\text{CJ}}^*(v_0) = D_{\text{CJ}}(v_0, p_0^*(v_0))$ and $s_{\text{CJ}}^*(v_0) = s_{\text{CJ}}(v_0, p_0^*(v_0))$ of v_0 , hence, from (38) and (39),

$$\frac{v_0}{D_{\text{CJ}}} \frac{dD_{\text{CJ}}^*}{dv_0} = F_{\text{CJ}}^{-1} \left(1 - \frac{v_{\text{CJ}}}{v_0} \right)^{-1} \Phi_{v_{\text{CJ}}}^*, \quad (45)$$

$$\frac{v_0 T_{\text{CJ}}}{D_{\text{CJ}}^2} \frac{ds_{\text{CJ}}^*}{dv_0} = F_{\text{CJ}}^{-1} \left(1 - \frac{v_{\text{CJ}}}{v_0} \right) \Phi_{v_{\text{CJ}}}^* + \Phi_{s_{\text{CJ}}}^*. \quad (46)$$

The slope dp_0^*/dv_0 is thus the parameter that determines how the initial and final properties vary with v_0 for initial states varying on $p_0^*(v_0)$ (Fig. 1). Final states varying at constant initial state lie on the same Hugoniot, initial states varying on $p_0^*(v_0)$ generate a $(p-v)$ arc of final states between a point U on a Hugoniot H with pole $O(v_0, p_0)$ and a point U' on another Hugoniot H' with pole $O'(v_0 + dv_0, p_0 + dp_0^*(v_0))$. The partial derivative $\partial\eta^*/\partial D|_{v_0}$ is the variation of η with respect to D along the same Hugoniot, $\partial\eta^*/\partial v_0|_D$ is the variation of η with respect to v_0 from one Hugoniot to another for piston speeds u_p (Subsect. III-A) chosen for each initial state on $p_0^*(v_0)$ that the final states have the same D , and $\partial D/\partial v_0|_{s^*}$ and $\partial\eta^*/\partial v_0|_{s^*}$ are variations with respect to v_0 for u_p such that the final states are on the same isentrope arc. The demonstration requires the partial derivative of v^* with respect to v_0 to be finite along an equilibrium isentrope: physical CJ velocities are finite, so are isentrope slopes at CJ points (Subsect. III-D).

C. Demonstration and interpretation

Differentials (42) and (41) define two constraints on partial derivatives of $s^*(D, v_0)$ and $v^*(D, v_0)$

$$\Phi_s^* \equiv \frac{v_0 T}{D^2} \frac{\partial s^*}{\partial v_0} \Big|_D = - \left(1 - \frac{v}{v_0} \right)^2 \frac{v_0}{D} \frac{\partial D}{\partial v_0} \Big|_{s^*}, \quad (47)$$

$$\Phi_v^* \equiv (M^{-2} - 1) \frac{\partial v^*}{\partial v_0} \Big|_D = \dots \\ \dots (M^{-2} - 1) \frac{\partial v^*}{\partial v_0} \Big|_{s^*} + F \left(1 - \frac{v}{v_0} \right) \frac{v_0}{D} \frac{\partial D}{\partial v_0} \Big|_{s^*}. \quad (48)$$

From here, the wave is assumed to be a true discontinuity ($v/v_0 \neq 1$), so (47) indicates that, regardless of M ,

$$\Phi_s^* \propto \frac{\partial s^*}{\partial v_0} \Big|_D = 0 \Leftrightarrow \frac{\partial D}{\partial v_0} \Big|_{s^*} = 0, \quad (49)$$

a consequence of the triple product rule,

$$\frac{\partial s^*}{\partial v_0} \Big|_D = - \frac{\partial s^*}{\partial D} \Big|_{v_0} \frac{\partial D}{\partial v_0} \Big|_{s^*} \quad (50)$$

since (42) is the two-variable differential of $s^*(D, v_0)$,

$$ds^* = \frac{\partial s^*}{\partial D} \Big|_{v_0} dD + \frac{\partial s^*}{\partial v_0} \Big|_D dv_0, \quad (51)$$

and $\partial s^*/\partial D|_{v_0} = \left(1 - \frac{v}{v_0} \right)^2 (D^2/T) \neq 0$ (23). Neither of equality in (49) is true in general (Subsect. III-A) but both are so for sonic detonation states ($M = 1$, $v/v_0 < 1$): (48) and (49) give, successively,

$$\Phi_v^{*(M=1)} \propto \frac{\partial D}{\partial v_0} \Big|_{s^*}^{(M=1)} = 0, \quad \Phi_s^{*(M=1)} \propto \frac{\partial s^*}{\partial v_0} \Big|_D^{(M=1)} = 0 \quad (52)$$

if $\partial v^*/\partial v_0|_D^{(M=1)}$ and $\partial v^*/\partial v_0|_{s^*}^{(M=1)}$ are finite, hence the DSI theorem (31) from (45)-(46) or (51),

$$(ds^*)^{(M=1)} \equiv ds_{\text{CJ}}^* = 0 \Leftrightarrow (dD)^{(M=1)} \equiv dD_{\text{CJ}}^* = 0. \quad (53)$$

Equivalently, combining $dv^*(s, v_0)$ and (21), or (47) and (48), gives

$$\frac{\partial v^*}{\partial v_0} \Big|_D = \frac{\partial v^*}{\partial v_0} \Big|_s + \frac{\partial v^*}{\partial s} \Big|_{v_0} \frac{\partial s^*}{\partial v_0} \Big|_D \Leftrightarrow \quad (54)$$

$$\Phi_s^* = \frac{M^{-2} - 1}{F} \left(1 - \frac{v}{v_0} \right) \left(\frac{\partial v^*}{\partial v_0} \Big|_s - \frac{\partial v^*}{\partial v_0} \Big|_D \right), \quad (55)$$

so $\Phi_s^{*(M=1)} = 0$ if $(\partial v^*/\partial v_0)_s - \partial v^*/\partial v_0|_D^{(M=1)}$ is finite, then $\partial D/\partial v_0|_{s^*}^{(M=1)} = 0$ from (47), and $\Phi_v^{*(M=1)} = 0$ from (48). Different initial states that generate the same CJ velocity thus generate different CJ states with the same entropy. This can also be obtained from dp (36): its coefficients have the same absolute value as those of dv (35) if $M = 1$. Appendix C proposes a model problem.

An interpretation in the $p-v$ plane (Fig. 1) considers the Hugoniot curves $p_{\text{H}}(v; p_0, v_0)$ (14) as a one-parameter family $y_{\text{H}}^*(p, v; v_0) = 0$ with parameter v_0 if their poles (p_0, v_0) are distributed on $p_0^*(v_0)$,

$$y_{\text{H}}^*(p, v; v_0) = \dots \\ \dots - h(p, v) + h_0(p_0^*, v_0) + \frac{1}{2}(p - p_0^*)(v_0 + v). \quad (56)$$

This family has an envelope if $p_0^*(v_0)$ satisfies the constraint obtained by setting to zero the partial derivative of $y_{\text{H}}^*(p, v; v_0)$ with respect to v_0

$$\frac{\partial y_{\text{H}}^*}{\partial v_0} \Big|_{p,v} = 0 \Leftrightarrow \frac{dp_0^*}{dv_0} = - \left(\frac{D}{v_0} \right)^2 \times \frac{1 - \frac{v}{v_0} + \frac{2M_0^{-2}}{G_0}}{1 - \frac{v}{v_0} + \frac{2}{G_0}}, \quad (57)$$

and this envelope is an isentrope if it is made up of sonic points, as the CJ-entropy differential (39) shows.

Similarly, the Rayleigh-Michelson lines (R) $p_{\text{R}}(v, D; p_0, v_0)$ (14) form a two-parameter family $y_{\text{R}}^*(p, v; D, v_0) = 0$, with parameters v_0 and D , if their poles (p_0, v_0) are distributed on $p_0^*(v_0)$,

$$y_{\text{R}}^*(p, v; D, v_0) = -p + p_0^* + \left(\frac{D}{v_0} \right)^2 (v_0 - v), \quad (58)$$

which reduces to a one-parameter (v_0) sub-family if D is a function of v_0 and p_0 such as D_{CJ} (25). Thus, with $D_{\text{CJ}}^*(v_0) = D_{\text{CJ}}(v_0, p_0^*(v_0))$, setting to zero the partial derivative of $y_{\text{R}}^*(p, v; D_{\text{CJ}}^*(v_0), v_0)$ with respect to v_0 gives the envelope constraint for the R lines

$$\left. \frac{\partial y_{\text{R}}^*}{\partial v_0} \right|_{p,v} = 0 \Leftrightarrow \frac{dp_0^*}{dv_0} = - \left(\frac{D_{\text{CJ}}^*}{v_0} \right)^2 \times \dots$$

$$\dots \left\{ 2 \frac{v_{\text{CJ}}}{v_0} - 1 + 2 \left(1 - \frac{v_{\text{CJ}}}{v_0} \right) \frac{v_0}{D_{\text{CJ}}^*} \frac{dD_{\text{CJ}}^*}{dv_0} \right\}, \quad (59)$$

which is an isentrope if it is made up of sonic points. This can be observed from

$$G \frac{v_0}{v} \frac{T ds_{\text{R}}}{D^2} = \frac{v_0 dp_0}{D^2} + \left(2 \frac{v}{v_0} - 1 \right) \frac{dv_0}{v_0} \dots$$

$$\dots + 2 \left(1 - \frac{v}{v_0} \right) \frac{dD}{D} + (M^{-2} - 1) \frac{dv}{v_0}, \quad (60)$$

obtained by combining the differentials of the R relation (32) and the $s(p, v)$ equation of state (4). The DSI theorem $dD_{\text{CJ}}^* = 0$ along an isentrope then gives

$$\frac{dp_0^*}{dv_0} = - \left(\frac{D_{\text{CJ}}^*}{v_0} \right)^2 \times \left(2 \frac{v}{v_0} - 1 \right). \quad (61)$$

An isentrope is thus the common envelope (Fig. 1) of families of equilibrium Hugoniot and Rayleigh-Michelson lines with initial states such that CJ detonations have the same velocity. The connection with Davis' implementation of the Inverse Method for condensed explosives [47] is discussed in subsection III-D.

D. Chapman-Jouguet supplemental properties

1. *CJ state and isentrope.* The initial-state variations dp_0 and dv_0 ensuring the invariances of D_{CJ} and s_{CJ} are the non-zero solutions to either 2×2 homogeneous systems $\{dD_{\text{CJ}} = 0 - ds_{\text{CJ}} = 0\}$ (38)-(39) or $\{\Phi_v^* = 0 - \Phi_s^* = 0\}_{\text{CJ}}$ (52): their determinants are proportional to each other because any of their 4 constraints is a linear combination of the other 3. Setting either to zero, or identifying the envelope constraints (57) and (61) to each other, gives the condition

$$G_0 x_{\text{CJ}}^2 + 2x_{\text{CJ}} - (1 - M_{0\text{CJ}}^{-2}) = 0, \quad (62)$$

$$x_{\text{CJ}} = 1 - \frac{v_{\text{CJ}}}{v_0} = \frac{v_0 (p_{\text{CJ}} - p_0)}{D_{\text{CJ}}^2} = \frac{u_{\text{CJ}}}{D_{\text{CJ}}}. \quad (63)$$

The compressive solution $v_{\text{CJ}}/v_0 < 1$, $p_{\text{CJ}}/p_0 > 1$ and (27) or (28) form the one-variable (D_{CJ}) representation

(30) of the CJ detonation state

$$v_{\text{CJ}}(D_{\text{CJ}}; v_0, p_0) = v_0 \frac{1 + G_0 - \sqrt{1 + G_0 (1 - M_{0\text{CJ}}^{-2})}}{G_0}, \quad (64)$$

$$p_{\text{CJ}}(D_{\text{CJ}}; v_0, p_0) = p_0 + \frac{D_{\text{CJ}}^2}{v_0} \frac{\sqrt{1 + G_0 (1 - M_{0\text{CJ}}^{-2})} - 1}{G_0}, \quad (65)$$

$$\gamma_{\text{CJ}}(D_{\text{CJ}}; v_0, p_0) = \dots$$

$$\dots \frac{1 + G_0 - \sqrt{1 + G_0 (1 - M_{0\text{CJ}}^{-2})}}{G_0 \frac{p_0 v_0}{c_0^2} M_{0\text{CJ}}^{-2} - 1 + \sqrt{1 + G_0 (1 - M_{0\text{CJ}}^{-2})}}. \quad (66)$$

Conversely, D_{CJ} is a function of one CJ variable, for example, p_{CJ} (65),

$$\left(\frac{D_{\text{CJ}}}{c_0} \right)^2 = \pi_{\text{CJ}} \left(1 + \frac{1}{2\pi_{\text{CJ}}} \right) \left(1 + \sqrt{1 + \frac{G_0}{\left(1 + \frac{1}{2\pi_{\text{CJ}}} \right)^2}} \right), \quad (67)$$

where $\pi_{\text{CJ}} = v_0 (p_{\text{CJ}} - p_0) / c_0^2$, or γ_{CJ} (66),

$$\left(\frac{D_{\text{CJ}}}{c_0} \right)^2 = \frac{1}{2} \frac{(\gamma_{\text{CJ}} + 1)^2}{\gamma_{\text{CJ}}^2 - 1 - G_0} \times \left\{ 1 - 2 \frac{1 + \frac{G_0}{\gamma_{\text{CJ}} + 1}}{\gamma_{\text{CJ}} + 1} \frac{\gamma_{\text{CJ}}}{\tilde{\gamma}_0} + \dots \right.$$

$$\left. \dots \sqrt{1 - 4 \frac{1 + \frac{G_0 - (1 + G_0) \frac{\gamma_{\text{CJ}}}{\tilde{\gamma}_0}}{\gamma_{\text{CJ}} + 1}}{\gamma_{\text{CJ}} + 1} \frac{\gamma_{\text{CJ}}}{\tilde{\gamma}_0}} \right\}, \quad (68)$$

where $\tilde{\gamma}_0 = c_0^2 / p_0 v_0$ and must not be confused with γ_0 , except for gases (Subsect. II-A). Relation (68) shows a large sensitivity of D_{CJ} to γ_{CJ} , as is more evident in the gas example (71) below. The identity

$$G_0 = \frac{\alpha_0 c_0^2}{C_{p_0}}, \quad \alpha_0 = \frac{1}{v_0} \frac{\partial v_0}{\partial T_0} \bigg|_{p_0}, \quad (69)$$

indicates that the necessary initial data are c_0 , C_{p_0} , and v_0 measured as a function of T_0 at constant p_0 so the coefficient of thermal expansion α_0 can be determined.

For ideal gases, c , C_p , α and γ are functions of $T = pv(W/R)$ only, $G = \gamma - 1$, $v = RT/pW$, $\alpha = 1/T$. Thus, for initially-ideal gases,

$$\gamma_{\text{CJ}}(D_{\text{CJ}}, p_0, T_0) = \sqrt{\frac{\gamma_0}{1 - \frac{\gamma_0 - 1}{\gamma_0} M_{0\text{CJ}}^{-2}}}, \quad (70)$$

$$D_{\text{CJ}}^2(\gamma_{\text{CJ}}, p_0, T_0) = \frac{1 - \gamma_0^{-1}}{1 - \frac{\gamma_0}{\gamma_{\text{CJ}}^2}} \times c_0^2, \quad (71)$$

$$\frac{D_{\text{CJ}}^2(p_{\text{CJ}}, p_0, T_0)}{v_0 p_{\text{CJ}}} = \left(1 - \left(1 - \frac{\gamma_0}{2} \right) \frac{p_0}{p_{\text{CJ}}} \right) \times \dots$$

$$\dots \left\{ 1 + \sqrt{1 + \frac{(\gamma_0 - 1) \left(1 - \frac{p_0}{p_{\text{CJ}}} \right)^2}{\left(1 - \left(1 - \frac{\gamma_0}{2} \right) \frac{p_0}{p_{\text{CJ}}} \right)^2}} \right\}. \quad (72)$$

The strong-shock limits ($M_{0\text{CJ}}^{-2} \ll 1$ or $p_0/p_{\text{CJ}} \ll 1$) of γ_{CJ} and D_{CJ}^2 are $\sqrt{\gamma_0}$ and $(1 + \sqrt{\gamma_0}) v_0 p_{\text{CJ}}$, respectively (their acoustic limits are γ_0 and c_0^2). The typical values $\gamma_0 = 1.3$, $c_0 = 330$ m/s and $D_{\text{CJ}} = 2000$ m/s give $\gamma_{\text{CJ}} = 1.144$, $\sqrt{\gamma_0} = 1.140$ and relative error $100 \times (\gamma_{\text{CJ}}/\sqrt{\gamma_0} - 1) = 0.316$ %. Relations (70)-(72) apply only to initially-ideal gases, but products can be non-ideal if p_0 is large enough.

The (p_0, v_0) pairs that generate the invariance D_{CJ} or s_{CJ} are solutions to the ordinary differential equation formed by substituting (64) for v in (57) or (61). The initial condition is a reference initial state (p_{0*}, v_{0*}) with known CJ velocity D_{CJ}^* . The particular solution is the polar curve $p_0^*(v_0)$ through (p_{0*}, v_{0*}) , which, substituted for p_0 in $v_{\text{CJ}}(D_{\text{CJ}}; v_0, p_0)$ (64) and $p_{\text{R}}(v, D; v_0, p_0)$ (13) gives

$$v_{\text{CJ}}^*(v_0) = v_{\text{CJ}}(v_0, p_0^*(v_0), D_{\text{CJ}}^*), \quad (73)$$

$$p_{\text{CJ}}^*(v_0) = p_0^*(v_0) + \frac{D_{\text{CJ}}^{*2}}{v_0} \left(1 - \frac{v_{\text{CJ}}^*(v_0)}{v_0}\right). \quad (74)$$

The isentrope $p_s^*(v)$ is generated by eliminating v_0 between $v_{\text{CJ}}^*(v_0)$ and $p_{\text{CJ}}^*(v_0)$, that is, by varying v_0 and representing $p_{\text{CJ}}^*(v_0)$ as a function of $v_{\text{CJ}}^*(v_0)$. Thus, v_0 can parameterize an isentrope of detonation products. This, however, necessitates C_{p0} , c_0 and v_0 in a sufficiently large (p_0, T_0) domain whereas calculating the CJ state from (64), (65) and (66) necessitates them for one initial state only.

Physically, the DSI theorem holds because isentropes have finite slopes, so the derivatives $\partial z^*/\partial v_0)_s$ and $\partial z^*/\partial v_0)_D$ are finite and non-zero at sonic points (Subsect. III-C). Formally, this is obtained by differentiating $c(s, v)$ (5) and the mass balance (9-a) written as $v = v_0 M(c/D)$,

$$\frac{dv}{v} = \frac{dv_0}{v_0} + \frac{dc}{c} + \frac{dM}{M} - \frac{dD}{D}, \quad (75)$$

$$dc = \left(\frac{\partial c}{\partial s}\right)_v ds + \left(\frac{\partial c}{\partial v}\right)_s dv, \quad (76)$$

hence, restricting variations to an isentrope,

$$\Gamma \frac{v_0}{v} \frac{\partial v}{\partial v_0}_s = 1 - \frac{v_0}{D} \frac{\partial D}{\partial v_0}_s + \frac{v_0}{M} \frac{\partial M}{\partial v_0}_s, \quad (77)$$

with Γ the fundamental derivative of hydrodynamics (8). The sonic condition $M = \text{const.} = 1$ and the DSI consequence $\partial D/\partial v_0)_{s^*}^{(M=1)} = 0$ (52-a), combined with (7), (1) and (9), then give

$$\left(\frac{\partial v^*}{\partial v_0}\right)_{s^*}^{(M=1)} = - \left(\frac{v_0}{D_{\text{CJ}}}\right)^2 \left(\frac{\partial p^*}{\partial v_0}\right)_{s^*}^{(M=1)} = \Gamma_{\text{CJ}}^{-1} \frac{v_{\text{CJ}}}{v_0}, \quad (78)$$

$$\frac{v_0}{D_{\text{CJ}}^2} \left(\frac{\partial h^*}{\partial v_0}\right)_{s^*}^{(M=1)} = -\Gamma_{\text{CJ}}^{-1} \left(\frac{v_{\text{CJ}}}{v_0}\right)^2, \quad (79)$$

$$\frac{v_0}{D_{\text{CJ}}} \left(\frac{\partial u^*}{\partial v_0}\right)_{s^*}^{(M=1)} = (1 - \Gamma_{\text{CJ}}^{-1}) \frac{v_{\text{CJ}}}{v_0}. \quad (80)$$

Therefore, the derivatives of v , p and h are finite and non-zero at a CJ point except if $\Gamma_{\text{CJ}} \rightarrow \infty$ and $\Gamma_{\text{CJ}} = 0$, respectively (the derivative of u is zero for $\Gamma_{\text{CJ}} = 1$), and the constraints $\partial v^*/\partial v_0)_{s^*}^{(M=1)} < \infty$ and $\partial v^*/\partial v_0)_D^{(M=1)} < \infty$ are equivalent to each other. In contrast, with z denoting v , p or h , the derivatives $\partial z^*/\partial D)_{v_0}^{(M=1)}$ are infinite (or $\partial D/\partial z^*)_{v_0}^{(M=1)} = 0$), as (24) shows. In the perfect-gas example (App. A), taking the partial derivative of $v(D; v_0, p_0)$ (A8) with respect to D moves the square-root term to the denominator, so $\lim_{D \rightarrow D_{\text{CJ}}} \partial v/\partial D)_{p_0, v_0} = -\infty$, whereas its partial derivative with respect to v_0 , with $p_0 = p_0^*(v_0)$, shows that $\lim_{D \rightarrow D_{\text{CJ}}} \partial v^*/\partial v_0)_D$ is finite if $\partial D/\partial v_0)_{s^*} = 0$.

The ratio $dD_{\text{CJ}}/ds_{\text{CJ}}$ is obtained by eliminating dp_0/dv_0 between (38) and (39). The non-homogeneous term is zero from (62), hence

$$\frac{D_{\text{CJ}} dD_{\text{CJ}}}{T_{\text{CJ}} ds_{\text{CJ}}} = \left(1 - \frac{v_{\text{CJ}}}{v_0}\right)^{-2} \left(1 - F_{\text{CJ}} \frac{1 + G_0 \left(1 - \frac{v_{\text{CJ}}}{v_0}\right)}{2 + G_0 \left(1 - \frac{v_{\text{CJ}}}{v_0}\right)}\right). \quad (81)$$

The partial derivatives of $D_{\text{CJ}}(v_0, p_0)$, and those of $D_{\text{CJ}}(T_0, p_0)$, are not independent since there are initial-state variations for which D_{CJ} is constant. This is implied by the triple product rule,

$$\left(\frac{\partial D_{\text{CJ}}}{\partial z_0}\right)_{p_0} = - \left(\frac{\partial p_0}{\partial z_0}\right)_{D_{\text{CJ}}} \left(\frac{\partial D_{\text{CJ}}}{\partial p_0}\right)_{z_0}, \quad (82)$$

where z_0 denotes either v_0 or T_0 . Hence, with $\partial p_0/\partial v_0)_{D_{\text{CJ}}}$ given by (57) or (61),

$$\frac{v_0}{D_{\text{CJ}}} \left(\frac{\partial D_{\text{CJ}}}{\partial v_0}\right)_{p_0} = \frac{D_{\text{CJ}}}{v_0} \left(\frac{\partial D_{\text{CJ}}}{\partial p_0}\right)_{v_0} \times \left(2 \frac{v_{\text{CJ}}}{v_0} - 1\right), \quad (83)$$

$$\begin{aligned} \frac{D_{\text{CJ}}}{v_0} \left(\frac{\partial D_{\text{CJ}}}{\partial p_0}\right)_{T_0} &= \frac{T_0}{D_{\text{CJ}}} \left(\frac{\partial D_{\text{CJ}}}{\partial T_0}\right)_{p_0} \times \dots \\ &\dots \frac{1 - (1 + \alpha_0 T_0 G_0) \left(2 \frac{v_{\text{CJ}}}{v_0} - 1\right) M_{0\text{CJ}}^2}{\left(2 \frac{v_{\text{CJ}}}{v_0} - 1\right) \alpha_0 T_0}, \end{aligned} \quad (84)$$

the latter being obtained from the former and the identities

$$\frac{T_0}{D_{\text{CJ}}} \left(\frac{\partial D_{\text{CJ}}}{\partial T_0}\right)_{p_0} = \alpha_0 T_0 \frac{v_0}{D_{\text{CJ}}} \left(\frac{\partial D_{\text{CJ}}}{\partial v_0}\right)_{p_0}, \quad (85)$$

$$\begin{aligned} \frac{D_{\text{CJ}}}{v_0} \left(\frac{\partial D_{\text{CJ}}}{\partial p_0}\right)_{T_0} &= \frac{v_0}{D_{\text{CJ}}} \left(\frac{\partial D_{\text{CJ}}}{\partial p_0}\right)_{v_0} - \dots \\ &\dots M_0^2 (1 + \alpha_0 T_0 G_0) \frac{v_0}{D_{\text{CJ}}} \left(\frac{\partial D_{\text{CJ}}}{\partial v_0}\right)_{p_0}. \end{aligned} \quad (86)$$

The variations of D_{CJ} with respect to T_0 at constant p_0 thus determine those with respect to p_0 at constant T_0 , and conversely. The 5 constraints above also apply to s_{CJ} since $\partial p_0/\partial z_0)_{D_{\text{CJ}}} = \partial p_0/\partial z_0)_{s_{\text{CJ}}}$.

2. *The Inverse Method (IM)*. A reminder on this method (Sect. 1) is helpful to discuss below the DSI theorem, and its application to liquid explosives in subsection IV-B. Manson [5] and Wood and Fickett [46] were the first to discuss several IM implementations depending on the pair of independent initial-state variables. The two options in this work are conveniently introduced from

$$\frac{dD_{\text{CJ}}}{D_{\text{CJ}}} = \frac{1 - F_{\text{CJ}}(1 - x_{\text{CJ}})}{F_{\text{CJ}}x_{\text{CJ}}} \frac{dv_0}{v_0} - \dots$$

$$\dots \frac{1 + (1 - F_{\text{CJ}})(1 - x_{\text{CJ}})}{F_{\text{CJ}}x_{\text{CJ}}^2} \frac{v_0 dp_0}{D_{\text{CJ}}^2} + \frac{2 - F_{\text{CJ}}}{F_{\text{CJ}}x_{\text{CJ}}^2} \frac{dh_0}{D_{\text{CJ}}^2} \quad (87)$$

obtained by setting $M = 1$ in dv (35) or dp (36), and with x_{CJ} given by (63) and F by (19).

The first one considers the same homogeneous explosive and the pair (T_0, p_0) . Measurements of $D_{\text{CJ}}(T_0, p_0)$ give the values of its partial derivatives, using $dh_0(p_0, v_0)$ (2) reduces (87) to the differential (38) of $D_{\text{CJ}}(v_0, p_0)$ (Subsect. 3.2), and eliminating F_{CJ} (or G_{CJ}) (19) between its coefficients then gives the CJ state as the solution $x_{\text{CJ}} < 1$ of

$$G_0 L x_{\text{CJ}}^2 + 2K x_{\text{CJ}} - (1 - M_{0\text{CJ}}^{-2}) = 0, \quad (88)$$

where L and K for $D_{\text{CJ}}(v_0, p_0)$ and $D_{\text{CJ}}(T_0, p_0)$ are

$$L = 1 + \frac{D_{\text{CJ}}}{v_0} \frac{\partial D_{\text{CJ}}}{\partial p_0} \bigg|_{v_0} - \frac{v_0}{D_{\text{CJ}}} \frac{\partial D_{\text{CJ}}}{\partial v_0} \bigg|_{p_0}$$

$$= 1 + \frac{D_{\text{CJ}}}{v_0} \frac{\partial D_{\text{CJ}}}{\partial p_0} \bigg|_{T_0} + \dots$$

$$\dots \frac{1 - M_{0\text{CJ}}^{-2} + \alpha_0 T_0 G_0}{\alpha_0 T_0 M_{0\text{CJ}}^{-2}} \frac{T_0}{D_{\text{CJ}}} \frac{\partial D_{\text{CJ}}}{\partial T_0} \bigg|_{p_0}, \quad (89)$$

$$K = 1 + M_{0\text{CJ}}^{-2} \frac{D_{\text{CJ}}}{v_0} \frac{\partial D_{\text{CJ}}}{\partial p_0} \bigg|_{v_0} - \frac{v_0}{D_{\text{CJ}}} \frac{\partial D_{\text{CJ}}}{\partial v_0} \bigg|_{p_0}$$

$$= 1 + M_{0\text{CJ}}^{-2} \frac{D_{\text{CJ}}}{v_0} \frac{\partial D_{\text{CJ}}}{\partial p_0} \bigg|_{T_0} + \frac{G_0 T_0}{D_{\text{CJ}}} \frac{\partial D_{\text{CJ}}}{\partial T_0} \bigg|_{p_0}, \quad (90)$$

through $dv_0(T_0, p_0)$ and $dh_0(T_0, p_0)$ (69). The IM relation (88) also writes

$$L (G_0 x_{\text{CJ}}^2 + 2x_{\text{CJ}} - (1 - M_{0\text{CJ}}^{-2})) - (1 - M_{0\text{CJ}}^{-2}) \times \dots$$

$$\dots \left((1 - 2x_{\text{CJ}}) \frac{\partial D_{\text{CJ}}}{\partial p_0} \bigg|_{v_0} - \frac{\partial D_{\text{CJ}}}{\partial v_0} \bigg|_{p_0} \right) = 0, \quad (91)$$

which shows that (88) reduces to the DSI relation (62) by demanding the partial derivatives of D_{CJ} to meet their DSI compatibility relation (83). It must be emphasized that any assumption on the derivatives of D_{CJ} such that L and K are both equal to 1 also reduces (88) to (62). Such assumptions are non-physical because they necessarily select the acoustic-limit solution, which is evident from the expressions of L and K and the DSI compatibility relation (83) or (84). Indeed, the DSI and the IM relations (62) and (88) have two CJ solutions, the physical

one $-M_{0\text{CJ}} > 1$, $D_{\text{CJ}} > c_0$, $0 < x_{\text{CJ}} < 1$ – and the acoustic limit $-M_{0\text{CJ}} = 1$, $D_{\text{CJ}} = c_0$, $x_{\text{CJ}} = 0$. For example, Manson [48] had noted the strong-shock limit $\sqrt{\gamma_0}$ of γ_{CJ} for the ideal gas (70) by neglecting both non-dimensional derivatives $\partial \ln D_{\text{CJ}} / \partial \ln p_0|_{T_0}$ and $\partial \ln D_{\text{CJ}} / \partial \ln T_0|_{p_0}$ of $D_{\text{CJ}}(T_0, p_0)$. This contradicts the distinguished limit required by the large values of $M_{0\text{CJ}}^2$ in the coefficients of $\partial \ln D_{\text{CJ}} / \partial \ln p_0|_{T_0}$ and $\partial \ln D_{\text{CJ}} / \partial \ln T_0|_{p_0}$ in (89).

The second option uses the pair (v_0, h_0) at constant p_0 . This can be obtained with a set of isometric mixtures [49], that is, with all the same atomic composition, and hence the same equilibrium equation of state, for any value of a composition parameter, denoted below by w_0 after [46]. Typically, w_0 is the total volume- or mass-fraction of all compounds added to the reference composition, so the initial and CJ properties of the reference explosive are then defined by $w_0 = 0$. Measurements of $h_0(T_0, w_0)$, $v_0(T_0, w_0)$ and $D_{\text{CJ}}(T_0, w_0)$ at constant p_0 give the values of their partial derivatives, setting $dp_0 = 0$ in (87) gives the differential of $D_{\text{CJ}}(v_0, h_0)$, and eliminating F_{CJ} between its coefficients then gives the CJ state as the solution $x_{\text{CJ}} < 1$ of

$$L x_{\text{CJ}}^2 + 2K x_{\text{CJ}} - 1 = 0, \quad (92)$$

where L and K for $D_{\text{CJ}}(v_0, h_0)$ and $D_{\text{CJ}}(T_0, w_0)$ are

$$L = \frac{D_{\text{CJ}}}{D_{\text{CJ}}} \frac{\partial D_{\text{CJ}}}{\partial h_0} \bigg|_{v_0, p_0} = \dots$$

$$\dots \frac{\frac{\omega_0 T_0}{D_{\text{CJ}}} \frac{\partial D_{\text{CJ}}}{\partial T_0} \bigg|_{w_0, p_0} - \frac{\alpha_0 T_0}{D_{\text{CJ}}} \frac{\partial D_{\text{CJ}}}{\partial w_0} \bigg|_{T_0, p_0}}{\omega_0 \frac{C_{p_0} T_0}{D_{\text{CJ}}^2} - \alpha_0 T_0 \Omega_0}, \quad (93)$$

$$K = 1 - \frac{v_0}{D_{\text{CJ}}} \frac{\partial D_{\text{CJ}}}{\partial v_0} \bigg|_{h_0, p_0} = \dots$$

$$\dots 1 + \frac{\frac{\Omega_0 D_{\text{CJ}}}{T_0} \frac{\partial D_{\text{CJ}}}{\partial T_0} \bigg|_{w_0, p_0} - \frac{C_{p_0} T_0}{D_{\text{CJ}}^2} \frac{\partial D_{\text{CJ}}}{\partial w_0} \bigg|_{T_0, p_0}}{\omega_0 \frac{C_{p_0} T_0}{D_{\text{CJ}}^2} - \alpha_0 T_0 \Omega_0}, \quad (94)$$

through the identities

$$\frac{dv_0}{v_0} = \alpha_0 T_0 \frac{dT_0}{T_0} + \omega_0 dw_0, \quad \omega_0 = \frac{1}{v_0} \frac{\partial v_0}{\partial w_0} \bigg|_{T_0, p_0}, \quad (95)$$

$$\frac{dh_0}{D^2} = \frac{C_{p_0} T_0}{D^2} \frac{dT_0}{T_0} + \Omega_0 dw_0, \quad \Omega_0 = \frac{1}{D^2} \frac{\partial h_0}{\partial w_0} \bigg|_{T_0, p_0}. \quad (96)$$

This option is more convenient than the first because generating sufficiently-large variations of p_0 may be uneasy and because it does not necessitate c_0 .

The main drawback of the IM is its limited accuracy, in particular because the partial derivatives of D_{CJ} are measured independently of each other and cumulate their experimental uncertainties (Subsect. IV-B). The CJ properties derived from the DSI theorem require only the value of D_{CJ} .

3. *Remarks.* The variables v_0 and h_0 viewed as independent at constant p_0 determine envelope conditions (subsect. III-C) on D and h_0 for the families of Rayleigh-Michelson (R) lines (13) and Hugoniot (H) curves (14), that is,

$$\frac{v_0}{D} \frac{dD}{dv_0} = \frac{1}{2} \frac{1 - 2\frac{v}{v_0}}{1 - \frac{v}{v_0}} \equiv 1 - \left(2 \frac{v_0(p - p_0)}{D^2} \right)^{-1}, \quad (97)$$

$$\frac{v_0}{D^2} \frac{dh_0}{dv_0} = \frac{1}{2} \left(1 - \frac{v}{v_0} \right) \equiv -\frac{1}{2} \frac{v_0(p - p_0)}{D^2}, \quad (98)$$

respectively. The constraints (97) and (60) show that a sonic ($M = 1$) envelope to R lines is an isentrope, which combined with (37) indeed returns the envelope condition (98) for the H curves. The constraint $ds_{CJ} = 0$ is satisfied but not the constraint $dD_{CJ} = 0$ because it would imply $v_{CJ}/v_0 = 1/2$, that is, $\gamma_{CJ} = 1$.

The DSI theorem $dD_{CJ} = 0 \Leftrightarrow ds_{CJ} = 0$ is physically valid only if p_0 is varied, even if p_0/p or $v_0 p_0/D^2$ are negligible, and for initial and final states described with two-variable equations of state $T = T(p, v)$.

Davis [47] thus implemented the IM for condensed explosives ($p_0/p \approx 10^{-5}$) such that specific energy e_0 and mass $\rho_0 = 1/v_0$ are independent, and built $D_{CJ}(e_0, \rho_0)$ from Kamlet's method REF. He calculated the particular poles $e_0^*(\rho_0)$ of Hugoniots with the same isentropic envelope, this isentrope and the CJ states. His relations (14) and (31) are equivalent to (97) and (98), respectively, since $e_0 = h_0$ if p_0 is neglected. Similarly, Nagayama and Kubota [50] derived an envelope constraint for the R lines. They considered linear laws $D_{CJ}(\rho_0)$ with a negligible dependency on e_0 . Their relations (13) and (14) for the CJ state are equivalent to (97), that is, to $x_{CJ} = 1/2K$ from (92) and (93).

The differentials of the Rankine-Hugoniot relations and the equations of state form a 2×2 homogeneous linear system for dp_0 and dv_0 (with dh_0 subject to (34)) for any invariant pair of final-state variables. Only the invariance of D_{CJ} and s_{CJ} produces a non-trivially null determinant, that is, non-zero dp_0 and dv_0 , and relation (62) is this annulment condition. For example, in the p - v plane, no non-zero dp_0 and dv_0 permit a focal point $dp_{CJ} = 0$ - $dv_{CJ} = 0$. This would imply $dh_{CJ} = 0$, since $h = h(p, v)$, and, from (32), $dD_{CJ} = 0$, which represents the R line through (p_0, v_0) .

Equilibrium compositions in homogeneous media are functions of T and p , so their variations are consistently included in those of a $T(p, v)$ equation of state, as induced by the differentiations above (Subsect. III-B). Further, there is no reason for different initial states to generate the same frozen final composition.

IV. APPLICATION TO GASEOUS OR LIQUID EXPLOSIVES

As for gaseous explosives (Subsect. IV-A), the DSI theorem and some CJ supplemental properties were analysed through chemical equilibrium calculations. Only ideal detonation products were investigated to avoid the uncertainties induced by equations of state, such as those of condensed explosives, calibrated from experiments that may not have achieved the strict CJ equilibrium (Sect. I). The calculations were done with the NASA computer program CEA [43]. As for liquid explosives (Subsect. IV-B), the analysis is a comparative discussion of the theoretical CJ pressures from (65) and values from experiments and the Inverse Method (Subsect. III-D).

A. Gaseous explosives with ideal final states

Tables I show numerical values of s_{CJ} and D_{CJ} for the four stoichiometric mixtures $CH_4 + 2 O_2$, $C_3H_8 + 5 O_2$, $CH_4 + 2$ Air and $H_2 + 0.5$ Air. Five (T_0, p_0) pairs with T_0 evenly spaced between 200 K and 400 K were used to represent a largest physical range; the third ($T_0 = 298.15$ K, $p_0 = 1$ bar) was chosen as the reference initial state (v_{0*}, p_{0*}) (subscript *, Subsect. III-C). The values of p_0 were determined by dichotomy for each T_0 so all entropies have the reference value s_{CJ}^* . The results were analysed based on the mean velocities \bar{D}_{CJ} , absolute and mean relative deviations $\Delta D_{CJ}/\bar{D}_{CJ}$ and $m_{D_{CJ}}$, in percent, and corrected standard deviations $\sigma_{D_{CJ}}$.

$$\bar{D}_{CJ} = \frac{1}{I} \sum_{i=1}^{I=5} D_{CJi}, \quad \left(\frac{\Delta D_{CJ}}{\bar{D}_{CJ}} \right)_i = 100 \times \frac{D_{CJi} - \bar{D}_{CJ}}{\bar{D}_{CJ}}, \quad (99)$$

$$m_{D_{CJ}} = \frac{1}{I} \sum_{i=1}^{I=5} \left| \frac{\Delta D_{CJ}}{\bar{D}_{CJ}} \right|_i, \quad \sigma_{D_{CJ}} = \sqrt{\sum_{i=1}^{I=5} \frac{(D_{CJi} - \bar{D}_{CJ})^2}{I - 1}}. \quad (100)$$

All $m_{D_{CJ}}$'s and $\sigma_{D_{CJ}}$'s are very small. In particular, all D_{CJ} 's are close to their mean values \bar{D}_{CJ} to $\mathcal{O}(0.1)$ % at most. The agreement is practically exact for $C_3H_8 + 5 O_2$. This suggests that an iterative minimization of both $\Delta D_{CJ}/\bar{D}_{CJ}$ and $\Delta s_{CJ}/\bar{s}_{CJ}$ should return values of $p_0(T_0)$, \bar{D}_{CJ} and \bar{s}_{CJ} that even better satisfy the theorem and eliminate the slight decreasing trend of D_{CJ} with increasing T_0 at constant s_{CJ}^* observed here. The $p_0(T_0)$ values and the results in table I can be seen as zeroth-order iterates, so the $(v_0(T_0), p_0)$ pairs well approximate the polar curve $p_0^*(v_0)$ through (v_{0*}, p_{0*}) (Subsect. III-C). It is easy, albeit tedious, to check that another reference than $T_0^* = 298.15$ K and $p_0^* = 1$ bar returns similarly small $m_{D_{CJ}}$'s and $\sigma_{D_{CJ}}$'s.

These small values were validated through a sensitivity analysis based on initial states very close to a reference *, and CEA's numerical accuracy as a criterion. Table II shows results for the $C_3H_8 + 5 O_2$ mixture with three

TABLE I. Joint invariances of CJ entropy s_{CJ} and velocity D_{CJ} : CJ-velocity mean value \bar{D}_{CJ} , absolute relative deviation $\Delta D_{\text{CJ}}/\bar{D}_{\text{CJ}}$, mean relative deviation $m_{D_{\text{CJ}}}$, and corrected standard deviation $\sigma_{D_{\text{CJ}}}$ of 4 mixtures.

$CH_4 + 2 O_2$		$m_{D_{\text{CJ}}} = 0.08 \%$		
$\bar{D}_{\text{CJ}} = 2389.7 \text{ m/s}$		$\sigma_{D_{\text{CJ}}} = 2.47 \text{ m/s}$		
T_0 (K)	p_0 (bar)	s_{CJ} (kJ/kg/K)	D_{CJ} (m/s)	$\frac{\Delta D_{\text{CJ}}}{\bar{D}_{\text{CJ}}}$ (%)
200.00	0.6284	<i>id.</i>	2392.9	0.13
250.00	0.8118	<i>id.</i>	2391.2	0.06
298.15*	1.0000*	12.6653*	2389.6	~ 0.00
350.00	1.2165	<i>id.</i>	2388.0	-0.07
400.00	1.4410	<i>id.</i>	2386.7	-0.12

$C_3H_8 + 5 O_2$		$m_{D_{\text{CJ}}} = 0.012 \%$		
$\bar{D}_{\text{CJ}} = 2356.7 \text{ m/s}$		$\sigma_{D_{\text{CJ}}} = 0.41 \text{ m/s}$		
T_0 (K)	p_0 (bar)	s_{CJ} (kJ/kg/K)	D_{CJ} (m/s)	$\frac{\Delta D_{\text{CJ}}}{\bar{D}_{\text{CJ}}}$ (%)
200.00	0.6304	<i>id.</i>	2357.3	0.03
250.00	0.8127	<i>id.</i>	2356.7	~ 0.00
298.15*	1.0000*	11.9293*	2356.3	-0.01 ₅
350.00	1.2165	<i>id.</i>	2356.3	-0.01 ₅
400.00	1.4419	<i>id.</i>	2356.7	~ 0.00

$CH_4 + 2 \text{ Air}$		$m_{D_{\text{CJ}}} = 0.05 \%$		
$\bar{D}_{\text{CJ}} = 1799.9 \text{ m/s}$		$\sigma_{D_{\text{CJ}}} = 1.23 \text{ m/s}$		
T_0 (K)	p_0 (bar)	s_{CJ} (kJ/kg/K)	D_{CJ} (m/s)	$\frac{\Delta D_{\text{CJ}}}{\bar{D}_{\text{CJ}}}$ (%)
200.00	0.6044	<i>id.</i>	1801.4	0.08
250.00	0.7968	<i>id.</i>	1800.7	0.05
298.15*	1.0000*	9.4218*	1799.9	~ 0.00
350.00	1.2401	<i>id.</i>	1799.1	-0.04
400.00	1.4949	<i>id.</i>	1798.3	-0.09

$H_2 + 0.5 \text{ Air}$		$m_{D_{\text{CJ}}} = 0.1 \%$		
$\bar{D}_{\text{CJ}} = 1964.7 \text{ m/s}$		$\sigma_{D_{\text{CJ}}} = 2.55 \text{ m/s}$		
T_0 (K)	p_0 (bar)	s_{CJ} (kJ/kg/K)	D_{CJ} (m/s)	$\frac{\Delta D_{\text{CJ}}}{\bar{D}_{\text{CJ}}}$ (%)
200.00	0.6004	<i>id.</i>	1967.9	0.16
250.00	0.7941	<i>id.</i>	1966.4	0.08
298.15*	1.0000*	10.5927*	1964.8	~ 0.00
350.00	1.2444	<i>id.</i>	1963.1	-0.08
400.00	1.5042	<i>id.</i>	1961.5	-0.16

groups of four (T_0, p_0) pairs. The first pairs (superscript *) are the firsts, thirds and fifths in table I-2, so they generate the same entropy s_{CJ}^* . Their CJ states were used as the references of their group. The seconds (italics) have T_0 's only 5 % greater than the firsts and p_0 's determined by dichotomy so that $s_{\text{CJ}} = s_{\text{CJ}}^*$. The $\Delta D_{\text{CJ}}/D_{\text{CJ}}^*$'s are thus at most equal to the $\mathcal{O}(10^{-2})$ -% $m_{D_{\text{CJ}}}$'s in table I-2, and smaller T_0 variations would be non-significant. The thirds and fourths are variations at constant T_0 and constant p_0 , respectively. In each group, the initial variations chosen to generate the same s_{CJ}^* (the seconds) give

the smaller variations of T_{CJ} , which all are all greater than CEA's $\mathcal{O}(10^{-3})$ -% accuracy $\tilde{d}T/T = \tilde{d}p/p = 0.005 \%$ ([43], p.35, eqs.7.24, and p.40) by at least one order of magnitude. The initial variations chosen not to generate the same entropy s_{CJ}^* (the thirds and fourths) give variations of D_{CJ} 10 times greater than $m_{D_{\text{CJ}}}$ and the same $\mathcal{O}(10^{-1})$ -% magnitudes for those of s_{CJ} and T_{CJ} . Therefore, the small $\mathcal{O}(10^{-2})$ -% variations of D_{CJ} at constant s_{CJ} , and the greater ones of s_{CJ} and D_{CJ} at constant T_0 and p_0 , are valid and not due to initial states chosen too close to each other. The variations of s_{CJ} are slightly smaller than those of T_{CJ} : the combination of $dh(s, p)$ (1), $dh(T) = C_p dT$ (3), $pv = RT/W$ and $\gamma = C_p/C_v$, subject to $\tilde{d}T/T = \tilde{d}p/p$, gives

$$\frac{\tilde{d}s}{s} = (2 - \gamma^{-1}) \frac{C_p}{s} \times \frac{\tilde{d}T}{T} = \mathcal{O}(10^{-1} - 1) \times \frac{\tilde{d}T}{T}, \quad (101)$$

since typical γ , s and C_p are $\mathcal{O}(1)$, $\mathcal{O}(10)$ kJ/K/kg and $\mathcal{O}(1-10)$ kJ/K/kg, respectively. At $p_0 = 1$ bar and $T_0 = 298.15$ K, CEA gives $\tilde{d}s_{\text{CJ}}/s_{\text{CJ}} = 0.33 \times \tilde{d}T_{\text{CJ}}/T_{\text{CJ}}$ for $CH_4 + 2 \text{ Air}$, and $\tilde{d}s_{\text{CJ}}/s_{\text{CJ}} = 0.89 \times \tilde{d}T_{\text{CJ}}/T_{\text{CJ}}$ for $CH_4 + 2 O_2$.

The theoretical (theo) ratios $(\rho_{\text{CJ}}/\rho_0, p_{\text{CJ}}/p_0, \gamma_{\text{CJ}}) \equiv r_{\text{CJ}}$ were calculated from (27), (28) and (70) using CEA values of D_{CJ} and the initial-state variables, and compared to CEA numerical (num) values. Tables III and IV show initial data and results for C_3H_8/O_2 mixtures with equivalence ratios $ER = 0.8, 1$ and 2 , $T_0 = 200$ K, 298.15 K and 400 K, and $p_0 = 0.2$ bar, 1 bar and 5 bar. Numbers are rounded, hence non-significant discrepancies between the indicated relative differences ϵ_r and those calculated from rounded $r_{\text{CJ}}^{(\text{num})}$ and $r_{\text{CJ}}^{(\text{theo})}$,

$$\epsilon_r = 100 \times \frac{r_{\text{CJ}}^{(\text{num})} - r_{\text{CJ}}^{(\text{theo})}}{r_{\text{CJ}}^{(\text{num})}}. \quad (102)$$

All ϵ_r 's are small, ranging from $\mathcal{O}(10^{-1})$ to $\mathcal{O}(1)$ %, but greater than the $\mathcal{O}(10^{-2} - 10^{-1})$ -% $m_{D_{\text{CJ}}}$'s, likely because of the sensitivity to the initial thermodynamic coefficients: the accuracy of C_{p_0} determines the others.

The uncertainties of s_{CJ} , γ_{CJ} , ρ_{CJ} and p_{CJ} are obtained from $ds(p, v)$ (1), (27), (28), $pv = RT/W$, $\gamma_{\text{CJ}}^2 \approx \gamma_0 = C_{p_0}/C_{v_0}$ (70) and $C_{p_0} - C_{v_0} = R/W_0$. The typical values $M_{0\text{CJ}}^{-2} \ll 1$, $\gamma_{\text{CJ}}^2 \approx \gamma_0 \approx G_{\text{CJ}} + 1 \approx 1.2$, $s_{\text{CJ}} \approx 10^4$ J/kg, $R \approx 8$ J/kg/mole, $W_{\text{CJ}} \approx 2 \times 10^{-2}$ kg/mole, and the Newtonian limit $\gamma_{\text{CJ}} \approx 1^+$, then give the estimates

$$\frac{\delta s_{\text{CJ}}}{s_{\text{CJ}}} = \frac{2}{s_{\text{CJ}} G_{\text{CJ}}} \frac{R}{W} \frac{1 - M_{0\text{CJ}}^{-2}}{1 + M_{0\text{CJ}}^{-2}/\gamma_0} \frac{\delta D_{\text{CJ}}}{D_{\text{CJ}}} \approx \frac{1}{10} \frac{\delta D_{\text{CJ}}}{D_{\text{CJ}}}, \quad (103)$$

$$\begin{aligned} \frac{\delta \gamma_{\text{CJ}}}{\gamma_{\text{CJ}}} &= \frac{1}{2} \left(1 + \frac{M_{0\text{CJ}}^{-2}/\gamma_0}{1 - \frac{\gamma_0 - 1}{\gamma_0} M_{0\text{CJ}}^{-2}} \right) \frac{\delta \gamma_0}{\gamma_0} \dots \\ &\dots + \frac{\frac{\gamma_0 - 1}{\gamma_0} M_{0\text{CJ}}^{-2}}{1 - \frac{\gamma_0 - 1}{\gamma_0} M_{0\text{CJ}}^{-2}} \frac{\delta D_{\text{CJ}}}{D_{\text{CJ}}} \approx \frac{1}{2} \frac{\delta \gamma_0}{\gamma_0} = \frac{\delta C_{p_0}}{C_{p_0}}, \quad (104) \end{aligned}$$

TABLE II. Joint invariances of CJ entropy s_{CJ} and velocity D_{CJ} : sensitivity to small changes of initial state of the $\text{C}_3\text{H}_8 + 5 \text{O}_2$ mixture.

T_0 (K)	p_0 (bar)	s_{CJ} (kJ/kg/K)	$\frac{\Delta s_{\text{CJ}}}{s_{\text{CJ}}^*}$ (%)	D_{CJ} (m/s)	$\frac{\Delta D_{\text{CJ}}}{D_{\text{CJ}}^*}$ (%)	T_{CJ} (K)	$\frac{\Delta T_{\text{CJ}}}{T_{\text{CJ}}^*}$ (%)
200.00*	0.6304*	11.9293*	/	2357.3*	/	3799.46*	/
210.00	0.6660	11.9293*	/	2357.1	-0.01	3801.57	0.06
200.00	0.6660	11.9093	-0.17	2359.7	0.10	3810.15	0.28
210.00	0.6304	11.9493	0.17	2354.7	-0.14	3790.91	-0.22
298.15*	1.0000*	11.9293*	/	2356.3*	/	3821.11*	/
313.06	1.0606	11.9293*	/	2356.3	0.00	3824.64	0.09
298.15	1.0606	11.9078	-0.18	2358.9	0.11	3832.68	0.30
313.06	1.0000	11.9508	0.18	2353.6	-0.11	3813.09	-0.21
400.00*	1.4419*	11.9293*	/	2356.7*	/	3846.74*	/
420.00	1.5371	11.9293*	/	2356.9	0.01	3852.19	0.14
400.00	1.5371	11.9059	-0.20	2359.6	0.12	3859.48	0.33
420.00	1.4419	11.9527	0.20	2354.0	-0.11	3839.46	-0.19

TABLE III. Initial data for calculating the theoretical CJ state from the CJ velocity D_{CJ} for $\text{C}_3\text{H}_8/\text{O}_2$ mixtures with 3 equivalence ratios ER and 3 initial temperatures T_0 and pressures p_0 (Table IV, theo).

T_0 (K)	p_0 (bar)	ER = 0.8				ER = 1				ER = 1.2			
		$W_0 = 33.667 \text{ (g/mol)}$				$W_0 = 34.015 \text{ (g/mol)}$				$W_0 = 34.340 \text{ (g/mol)}$			
		γ_0	c_0 (m/s)	v_0 (m ³ /kg)	D_{CJ} (m/s)	γ_0	c_0 (m/s)	v_0 (m ³ /kg)	D_{CJ} (m/s)	γ_0	c_0 (m/s)	v_0 (m ³ /kg)	D_{CJ} (m/s)
200.	0.2	<i>id.</i>	<i>id.</i>	2.4696	2203.9	<i>id.</i>	<i>id.</i>	2.4444	2306.7	<i>id.</i>	<i>id.</i>	2.4212	2392.0
	1	1.3390	257.2	0.4939	2269.8	1.3286	254.9	0.4889	2377.6	1.3194	252.8	0.4842	2466.1
	5	<i>id.</i>	<i>id.</i>	0.0988	2334.7	<i>id.</i>	<i>id.</i>	0.0978	2447.5	<i>id.</i>	<i>id.</i>	0.0968	2538.8
298.15	0.2	<i>id.</i>	<i>id.</i>	3.6816	2182.5	<i>id.</i>	<i>id.</i>	3.6439	2284.6	<i>id.</i>	<i>id.</i>	3.6094	2369.8
	1	1.3061	310.1	0.7363	2249.2	1.2924	306.9	0.7288	2356.3	1.2807	304.1	0.7219	2444.7
	5	<i>id.</i>	<i>id.</i>	0.1473	2315.4	<i>id.</i>	<i>id.</i>	0.1458	2427.6	<i>id.</i>	0.000.0	0.1444	2518.9
400.	0.2	<i>id.</i>	<i>id.</i>	4.9393	2165.5	<i>id.</i>	<i>id.</i>	4.8887	2267.6	<i>id.</i>	<i>id.</i>	4.8425	2352.9
	1	1.2716	354.4	0.9878	2233.2	1.2563	350.5	0.9777	2340.1	1.2434	347.0	0.9685	2428.6
	5	<i>id.</i>	<i>id.</i>	0.1976	2300.6	<i>id.</i>	<i>id.</i>	0.1956	2412.6	<i>id.</i>	<i>id.</i>	0.1937	2504.2

$$\begin{aligned} \frac{\delta \rho_{\text{CJ}}}{\rho_{\text{CJ}}} &= \frac{-1}{\gamma_{\text{CJ}} + 1} \frac{\delta \gamma_{\text{CJ}}}{\gamma_{\text{CJ}}} + \frac{2M_{0\text{CJ}}^{-2}/\gamma_0}{1 + M_{0\text{CJ}}^{-2}/\gamma_0} \frac{\delta D_{\text{CJ}}}{D_{\text{CJ}}} \\ &\approx \frac{-1}{4} \frac{\delta \gamma_0}{\gamma_0} = \frac{-1}{2} \frac{\delta C_{p_0}}{C_{p_0}}, \end{aligned} \quad (105)$$

$$\begin{aligned} \frac{\delta p_{\text{CJ}}}{p_{\text{CJ}}} &= \frac{-\gamma_{\text{CJ}}}{\gamma_{\text{CJ}} + 1} \frac{\delta \gamma_{\text{CJ}}}{\gamma_{\text{CJ}}} + \frac{2}{1 + M_{0\text{CJ}}^{-2}/\gamma_0} \frac{\delta D_{\text{CJ}}}{D_{\text{CJ}}} \\ &\approx \frac{-1}{4} \frac{\delta \gamma_0}{\gamma_0} = \frac{-1}{2} \frac{\delta C_{p_0}}{C_{p_0}}. \end{aligned} \quad (106)$$

The first shows that D_{CJ} is 10 times more sensitive than s_{CJ} , which validates the choice above of analysing the DSI theorem with initial states generating the same s_{CJ} rather than the same D_{CJ} . The next three show that γ_{CJ} is twice more sensitive than ρ_{CJ} and p_{CJ} , with p_{CJ} slightly more so than ρ_{CJ} (Table IV). The same is true for other mixtures: $\epsilon_\gamma = -3.4 \%$ and $m_{D_{\text{CJ}}} = 0.08 \%$ for $\text{CH}_4 + 2 \text{O}_2$ at $T_0 = 298.15 \text{ K}$ and $p_0 = 1 \text{ bar}$. The uncertainty of γ_{CJ} is twice as small as that of γ_0 , as (70) shows, and thus the same as that of C_{p_0} . The magnitude of $\delta C_{p_0}/C_{p_0}$ depends on T_0 , p_0 and the components and proportions of the mixture; a sensitivity study to thermochemical databases should be carried out.

These calculations support physically and numerically the DSI theorem in a large range of initial conditions: the larger $\Delta D_{\text{CJ}}/\bar{D}_{\text{CJ}}$'s at constant s_{CJ} are very small, smaller than at constant p_0 or T_0 , and not numerical uncertainties. They also support the CJ supplemental properties: their differences with the numerical values is very small, and smaller than the physical uncertainty of thermochemical coefficients. The five fuels CH_4 , C_2H_2 , C_2H_4 , C_2H_6 and H_2 show similar trends.

B. Liquid explosives

Four liquids were investigated, namely nitromethane (NM, CH_3NO_2), isopropyl nitrate (IPN, $\text{C}_3\text{H}_7\text{NO}_3$), hot trinitrotoluene (TNT, $\text{C}_7\text{H}_5\text{N}_3\text{O}_6$), and the stoichiometric mixture made up of 1 volume of 2-nitropropane (NP, $\text{C}_3\text{H}_7\text{NO}_2$) and 3 volumes of nitric acid (NA, HNO_3), referred to below as niprona (NPNA3 $\text{C}_3\text{H}_{10}\text{N}_4\text{O}_{11}$). Table V compares their theoretical CJ detonation pressures (65) and adiabatic exponents (66) (theo), calculated using experimental detonation velocities, to measured values (exp) and those given by the

TABLE IV. Comparison of numerical (num) and theoretical (theo) CJ properties (r_{CJ}) for C_3H_8/O_2 mixtures with 3 equivalence ratios ER and 3 initial temperatures T_0 and pressures p_0 .

T_0 (K)	p_0 (bar)	r_{CJ}	ER = 0.8			ER = 1			ER = 1.2		
			num	theo	ϵ_r (%)	num	theo	ϵ_r (%)	num	theo	ϵ_r (%)
200.	0.2	ρ_{CJ}/ρ_0	1.870	1.844	1.38	1.870	1.849	1.14	1.870	1.854	0.86
		p_{CJ}/p_0	46.746	46.010	1.58	51.635	50.966	1.29	55.950	55.402	0.98
		γ_{CJ}	1.125	1.159	-3.03	1.127	1.154	-2.41	1.130	1.150	-1.81
	1	ρ_{CJ}/ρ_0	1.864	1.845	1.02	1.865	1.850	0.77	1.863	1.855	0.47
		p_{CJ}/p_0	49.354	48.775	1.17	54.602	54.121	0.88	59.180	58.861	0.54
		γ_{CJ}	1.134	1.159	-2.23	1.136	1.154	-1.60	1.139	1.150	-0.96
	5	ρ_{CJ}/ρ_0	1.859	1.846	0.69	1.859	1.851	0.43	1.858	1.856	0.11
		p_{CJ}/p_0	51.990	51.580	0.79	57.612	57.325	0.50	62.436	62.357	0.13
		γ_{CJ}	1.142	1.159	-1.50	1.144	1.154	-0.86	1.148	1.150	-0.19
298.15	0.2	ρ_{CJ}/ρ_0	1.861	1.844	0.92	1.863	1.852	0.58	1.863	1.858	0.27
		p_{CJ}/p_0	30.939	30.617	1.04	34.170	33.947	0.65	37.031	36.919	0.30
		γ_{CJ}	1.123	1.146	-1.98	1.125	1.139	-1.23	1.128	1.134	-0.53
	1	ρ_{CJ}/ρ_0	1.856	1.846	0.55	1.857	1.854	0.20	1.857	1.860	-0.12
		p_{CJ}/p_0	32.696	32.491	0.63	36.165	36.084	0.23	39.206	39.262	-0.14
		γ_{CJ}	1.132	1.145	-1.18	1.134	1.139	-0.43	1.137	1.134	0.32
	5	ρ_{CJ}/ρ_0	1.852	1.848	0.20	1.852	1.855	-0.16	1.852	1.861	-0.50
		p_{CJ}/p_0	34.486	34.406	0.23	38.204	38.273	-0.18	41.418	41.654	-0.57
		γ_{CJ}	1.140	1.145	-0.43	1.143	1.139	0.34	1.146	1.133	1.11
400.	0.2	ρ_{CJ}/ρ_0	1.852	1.845	0.38	1.855	1.855	-0.00	1.855	1.862	-0.39
		p_{CJ}/p_0	22.843	22.747	0.42	25.232	25.233	-0.00	27.352	27.471	-0.43
		γ_{CJ}	1.122	1.131	-0.79	1.124	1.124	-0.04	1.126	1.117	0.79
	1	ρ_{CJ}/ρ_0	1.848	1.848	-0.01	1.850	1.857	-0.39	1.850	1.864	-0.78
		p_{CJ}/p_0	24.162	24.164	-0.01	26.726	26.843	-0.44	28.982	29.238	-0.88
		γ_{CJ}	1.131	1.131	-0.01	1.133	1.123	0.85	1.136	1.117	1.63
	5	ρ_{CJ}/ρ_0	1.843	1.850	-0.36	1.845	1.859	-0.76	1.845	1.866	-1.17
		p_{CJ}/p_0	25.512	25.618	-0.41	28.262	28.505	-0.86	30.652	31.059	-1.33
		γ_{CJ}	1.139	1.131	0.77	1.142	1.123	1.62	1.145	1.117	2.43

Inverse Method (IM, Subsect. III-D). Tables VI and VII show the sensitivity of the IM results to the uncertainties of the initial data and the velocity derivatives for NM and IPN. The IM results in table V were obtained with the average derivatives of $D_{CJ}^{(exp)}$ (second lines and columns, respectively, tabs. VI and VII). All theoretical pressures in table V are significantly greater than the experimental and the IM pressures. The low theoretical γ_{CJ} are consistent with the large p_{CJ} . However, tables VI and VII indicate that the theoretical and the IM values can agree with each other. The analysis below of these disparate trends is a speculative disentanglement of uncertainties and physics.

The initial-state data are ancient, but reliable and still referred to, e.g. [51] and [52] for IPN. However, they can vary slowly over time, so their detonation properties too. No references here ensure that measurements were carried out with the same batches of explosives over short enough periods. For NM, four data sets – *I*, *II*, *III*, *IV* – at $T_0 = 4$ C and $p_0 = 1$ bar were thus used to assess the sensitivity of the calculations to small initial-state variations. For NM *I*, they were taken in Brochet and Fisson [53], and for NM *II* in Davis, Craig and Ramsay [54] except for c_0 taken in [53]. For NM *III*, the initial properties are those in Lysne and Hardesty [55] except for C_{p_0} calculated with the fit $C_{p_0}(\text{J/kg/K})$

$= 1720.9 + 0.54724 \times T_0(\text{C})$ of Jones and Giauque’s measurements [56] between the melting (245 K) and ambient (298 K) temperatures; the CJ properties are those in [53]. For NM *IV*, ρ_0 and α_0 were calculated with the fit $\rho_0(\text{kg/m}^3) = 1152.0 - 1.1395 \times T_0(\text{C}) - 1.665 \times 10^{-3} \times T_0^2(\text{C})$ in Berman and West [57]. For IPN, the data were taken in [53], for NPNA3 in Bernard, Brossard, Claude and Manson [58], and for TNT in [54] and [59] except for c_0 identified to the constant a of the linear asymptote $D = a + bu$ to Garn’s shock Hugoniot measurements [60]. The derivatives of $D_{CJ}^{(exp)}$ necessary to implement the Inverse Method could be found only for NM and IPN. Tables VI and VII-right show those of $D_{CJ}^{(exp)}(T_0, p_0)$ for NM and IPN from [53]. Table VII-left shows those of $D_{CJ}^{(exp)}(T_0, w_0)$ for NM from [54], obtained from isometric mixtures of NM and acenina at mass fractions w_0 . Acenina is defined in [54] as the equimolar mixture of methyl cyanide (CH_3CN), nitric acid (HNO_3) and water, so its atomic composition is proportional to that of NM (CH_3NO_2).

For NM, the theoretical pressures are insensitive to the uncertainties of the initial state (Tab. V), unlike the (T_0, p_0) -IM pressures (Tab. VI), which can agree with the former: the same $p_{CJ} = 17.9$ GPa is obtained with the values $\rho_0 = 1149$ kg/m³ and $\alpha_0 = 1.023$

TABLE V. Comparison of CJ detonation pressures and adiabatic exponents (exp: experiments, IM: Inverse Method (IM), theo: CJ supplemental properties) at $p_0 = 1$ bar for nitromethane (NM), isopropyl nitrate (IPN), niprona (NPNA3), and trinitrotoluene (TNT). Symbol \emptyset : no data.

	T_0 (C)	ρ_0 (kg/m ³)	$\alpha_0 \times 10^3$ (1/K)	C_{p_0} (J/kg/K)	c_0 (m/s)	G_0	$D_{CJ}^{(exp)}$ (m/s)	p_{CJ} (GPa)			γ_{CJ}		
								exp	IM	theo	exp	IM	theo
<i>I</i>	4	1156	1.19	1747	1423	1.38	6330	12.7	12.9	17.5	2.65	2.58	1.65
NM <i>II</i>	4	1159	1.16	1733	1423	1.36	6334	14.8	12.6	17.6	2.14	2.69	1.65
<i>III</i>	4	1151	1.22	1723	1400	1.39	6330	12.7	13.6	17.4	2.63	2.39	1.65
<i>IV</i>	4	1147	1.00	1723	1400	1.14	6330	12.7	15.8	17.9	2.62	1.90	1.57
IPN	40	1017	1.23	1867	1049	0.72	5330	08.7	13.1	12.1	2.32	1.21	1.40
NPNA3	25	1275	1.11	1512	1184	1.03	6670	\emptyset	14.1	22.8	\emptyset	3.02	1.49
TNT	93	1450	0.70	1573	2140	2.04	6590	18.2	\emptyset	21.1	2.46	\emptyset	2.00

TABLE VI. Sensitivity of the Inverse-Method pressures p_{CJ}^{IM} (GPa) and adiabatic exponents γ_{CJ}^{IM} to the uncertainties of derivatives of measured detonation velocities $D_{CJ}^{(exp)}(T_0, p_0)$ and the initial data (Table V) for nitromethane (NM) at $T_0 = 277$ K and $p_0 = 1$ bar.

$\partial D_{CJ}^{(exp)}/\partial p_0)_{T_0}$ ± 0.01 (m/s/bar)		$\partial D_{CJ}^{(exp)}/\partial T_0)_{p_0} \pm 0.18$ (m/s/K)											
		-4.14				-3.96				-3.78			
		<i>I</i>	<i>II</i>	<i>III</i>	<i>IV</i>	<i>I</i>	<i>II</i>	<i>III</i>	<i>IV</i>	<i>I</i>	<i>II</i>	<i>III</i>	<i>IV</i>
0.19	p_{CJ}^{IM}	16.1	16.5	17.8	/	14.4	14.7	15.4	19.0	13.2	13.4	13.9	16.1
	γ_{CJ}^{IM}	1.87	1.81	1.59	/	2.22	2.17	2.00	1.40	2.50	2.46	2.32	1.85
0.20	p_{CJ}^{IM}	14.0	14.3	15.0	18.5	12.9	13.2	13.6	15.8	12.1	12.3	12.6	14.3
	γ_{CJ}^{IM}	2.30	2.25	2.08	1.48	2.58	2.53	2.39	1.90	2.83	2.79	2.66	2.22
0.21	p_{CJ}^{IM}	12.7	12.9	13.3	15.5	11.9	12.1	12.4	14.0	11.3	11.4	11.6	13.0
	γ_{CJ}^{IM}	2.65	2.61	2.46	1.96	2.89	2.85	2.72	2.28	3.12	3.08	2.96	2.54

TABLE VII. Sensitivity of the Inverse-Method pressures p_{CJ}^{IM} (GPa) and adiabatic exponents γ_{CJ}^{IM} to the uncertainties of derivatives of measured detonation velocities. **Left:** $D_{CJ}^{(exp)}(T_0, w_0)$ for nitromethane (NM *II*) at $T_0 = 277$ K and $p_0 = 1$ bar, acenina mass fraction $w_0 = 0$, $\partial h_0/\partial w_0)_{T_0, p_0} = (-2.021 \pm 0.17) \times 10^6$ (J/kg), $\partial v_0/\partial w_0)_{T_0, p_0} = (1.5 \pm 0.2) \times 10^{-3}$ (m³/kg). **Right:** $D_{CJ}^{(exp)}(T_0, p_0)$ for isopropyl nitrate (IPN) at $T_0 = 313$ K and $p_0 = 1$ bar. Symbol /: no solution to (88).

$\partial D_{CJ}^{(exp)}/\partial w_0)_{T_0, p_0}$ $\pm 0.18 \times 10^6$ (m ² /s ²)		$\partial D_{CJ}^{(exp)}/\partial T_0)_{w_0, p_0} \pm 0.18$ (m/s/K)			$\partial D_{CJ}^{(exp)}/\partial p_0)_{T_0}$ ± 0.10 (m/s/bar)		$\partial D_{CJ}^{(exp)}/\partial T_0)_{p_0} \pm 0.10$ (m/s/K)		
		-4.14	-3.96	-3.78			-4.13	-4.03	-3.93
-8.16	p_{CJ}^{IM}	12.4	12.6	12.7	0.2	p_{CJ}^{IM}	/	/	/
	γ_{CJ}^{IM}	2.74	2.70	2.66		γ_{CJ}^{IM}	/	/	/
-7.98	p_{CJ}^{IM}	12.5	12.6	12.7	0.3	p_{CJ}^{IM}	15.9	13.1	11.8
	γ_{CJ}^{IM}	2.73	2.69	2.65		γ_{CJ}^{IM}	< 1	1.21	1.45
-7.80	p_{CJ}^{IM}	12.5	12.7	12.8	0.4	p_{CJ}^{IM}	7.3	7.2	7.0
	γ_{CJ}^{IM}	2.72	2.67	2.63		γ_{CJ}^{IM}	2.94	3.03	3.12

K⁻¹ between those of NM *III* and *IV*, and with the values of derivatives $\partial D_{CJ}^{(exp)}/\partial T_0 = -3.96$ m/s/K and $\partial D_{CJ}^{(exp)}/\partial p_0 = 0.191 \times 10^{-5}$ m/s/bar contained in their confidence intervals. In contrast, the (T_0, w_0) -IM pressures (Tab. VII-left) are insensitive to the uncertainties of the initial state (not shown for concision). The differences are thus more likely due to the the physical assumptions of the model or the conditions of the measurements.

Davis, Craig and Ramsay [54],[30] refuted the CJ-equilibrium hypothesis for condensed explosives because their (T_0, w_0) -IM implementation for NM and TNT predicted smaller pressures than experiments. But Petrone [61] considered their interpretation of measurements

overestimated the experimental pressures: for NM at 4 C, they retained 14.8 GPa (Tab. V, NM *II*) instead of the values 12 – 14 GPa produced by most measurements and both the (T_0, p_0) - and (T_0, w_0) -IM implementations with their average velocity derivatives (Tabs. VI, excl. NM *IV*, and VII-left). However, the (T_0, p_0) -IM implementation for NM *III* also produces 14.8 GPa with values of velocity derivatives contained in their confidence intervals (Tab. VI), that is, $\partial D_{CJ}^{(exp)}/\partial T_0 = -4.12$ m/s/K and $\partial D_{CJ}^{(exp)}/\partial p_0 = 0.2 \times 10^{-5}$ m/s/bar. Equally important, the theoretical and the (T_0, p_0) -IM pressures can be equal to each other: for NM *III*, the theoretical pressure 17.4 GPa is obtained with the values of deriva-

tives $\partial D_{\text{CJ}}^{(\text{exp})}/\partial T_0 = -4.12 \text{ m/s/K}$ and $\partial D_{\text{CJ}}^{(\text{exp})}/\partial p_0 = 0.1902 \times 10^{-5} \text{ m/s/bar}$ that both belong to their confidence intervals and satisfy their DSI compatibility relationship (84). In contrast, the (T_0, w_0) -IM pressures are not very sensitive to the derivatives of $D_{\text{CJ}}^{(\text{exp})}(T_0, w_0)$ (Tab. VII-left), and are smaller than the theoretical values. The velocity derivatives are thus too scarce and imprecise to soundly discuss the CJ hypothesis from the IM pressures. Overall, the theoretical CJ pressures are greater than the measured values and most IM estimates, with differences greater than the typical experimental uncertainty $\pm 10 \text{ kbar}$ and small sensitivity to the initial data.

The velocities $D_{\text{CJ}}^{(\text{exp})}$ are linear extrapolations to infinite diameters of values measured in finite-diameter tubes and may not be CJ-equilibrium. The question is how large diameters should be so D_{CJ} is not underestimated or the propagation regime not sonic-frozen, perhaps even low-velocity. There are many analyses of the diameter effect in condensed explosives (Sect. I). Chiquete and Short [62] recently showed that characteristics originating from the explosive-tube interface can intersect the frozen sonic surface on its side opposite to the curved leading shock. The CJ-equilibrium detonation, or equivalently the TZD self-similar equilibrium expansion (Subsect. III-A) at the end of the ZND steady planar reaction zone, can thus be a hydrodynamic limit difficult to reach in condensed explosives: the flow is always diverging at the cylinder edge. This is consistent with Sharpe's numerical simulations of ignition by an overdriven detonation with a one-step reversible reaction rate [7]. In the long-time limit, the stable reaction zone relaxes to CJ-equilibrium for the planar wave, but to sonic frozen states for the spherically-diverging wave. The pressure measurements, for example through flyer-impact or Doppler-velocimetry techniques, cannot be discussed here, except to remind that a slope discontinuity on an experimental profile may not be a CJ-equilibrium locus and that extracting such a discontinuity from the signal noise can be difficult. The theory of hyperbolic equations, such as Euler's balance relations for inviscid fluids, ensures it is a sonic front, but probably frozen, as for the diameter effect. Detonation tubes at least should be as wide and long as possible, but the longer they are, the smaller the jump of derivatives of the TZD and the ZND flows at the sonic locus is, so the more difficult its detection is: the TZD derivatives tend towards zero with increasing detonation run distance, as do physical ZND derivatives with decreasing distance to the reaction-zone end.

At least one of the physical assumptions may thus not be satisfied, which include front adiabaticity, local thermodynamic equilibrium, equilibrium reaction-end states, and single-phase fluid (Sect. I).

One cause can be the two-step decomposition of the NO_2 grouping. In the compact semi-developed form, NM writes: $\text{CH}_3(\text{NO}_2)$, IPN: $(\text{CH}_3)_2(\text{H})\text{CO}(\text{NO}_2)$, TNT: $\text{C}_6\text{H}_2(\text{CH}_3)(\text{NO}_2)_3$, NP: $\text{C}(\text{CH}_3)_2(\text{H})(\text{NO}_2)$, and NA: $\text{O}(\text{H})(\text{NO}_2)$, so NPNA3 comprises 4 NO_2 groupings per

volume of NP. In gases, NO_2 first decomposes into NO which then decomposes into N_2 (cf. refs. in [26]). Branch et al [63] observed a two-front laminar flame in $\text{CH}_4/\text{NO}_2/\text{O}_2$ and $\text{CH}_2\text{O}/\text{NO}_2/\text{O}_2$ mixtures on a flat burner. Presles et al [64] evidenced a double cellular structure of detonation in gaseous NM, the transverse waves of the smaller cells propagating on the fronts of the larger cells. The first step gives the lower flame front and the smaller detonation cells. Whether the same process also applies to liquids is uncertain, but a weak flow divergence of the detonation zone may slowdown reaction sufficiently for the expansion head to enter the reaction zone and position at the intermediate decomposition step (Sect. II). Non-ideal self-sustained detonation regimes resulting from multi-step heat releases, possibly low-velocity, with pressures below CJ values are a well-known phenomenon in detonation physics REF.

Another cause can be the condensation of solid carbon, e.g. [18–23]. NM, TNT and IPN have negative oxygen balances, hence a large yield of carbon ($\approx 15\%$ in mass for NM). However, NPNA3 is stoichiometric, and yet all four liquids have theoretical CJ pressures greater than measured values. The condensation can select CJ-frozen states with pressures smaller than the CJ-equilibrium value (Sect. I), and the condensates can have speeds slower than the gas flow due to drag effects. This physical process likely begins before the chemical processes achieve sonic equilibrium. A (T, p) two-variable equilibrium equation of state and a single material speed might thus not be valid assumptions for these carbonate explosives.

These possibilities are not mutually exclusive. They suggest carrying out experiments in explosive cylinders wider and longer than usual and modelling based on multi-phase balance laws and constitutive relations with explicit thermal and mechanical non-equilibrium.

V. DISCUSSION AND CONCLUSIONS

This work brought out two new features of the CJ-equilibrium model of detonation. They are valid if the initial and burnt states are single-phase fluids at local and chemical equilibrium, with temperature T and pressure p as the independent state variables. The first one is that the CJ velocity and specific entropy are invariant under the same variations of the initial temperature and pressure (Subsect. III-C). The second one is essentially a set of relations for calculating the CJ state, including the adiabatic exponent, from the value of the CJ velocity, or the CJ velocity from one CJ variable (Subsect. III-D), that does not involve an equation state of detonation products. Therefore, they are not substitutes for detailed thermochemical numerical calculations (Sect. I) that give the CJ state, velocity and composition based on explicit (T, p) equilibrium equations of state, such as BKW and JCZ3, and their developments or reparametrizations, for condensed explosives [65, 66]. This justifies the question

as to what if anything has been gained in comparison to the usual methodology of measuring a pair of variables, such as pressure and velocity, to calibrate equations of state through numerical CJ calculations. Essentially, a simple semiempirical criterion is proposed to discuss whether a given pair can represent the CJ-equilibrium state, and thus to improve the measurement conditions or the modelling assumptions.

They compare accurately to calculations with detailed chemical equilibrium for detonation products described as ideal gases (Subsect. IV-A). However, they produce pressures larger than measured values for four carbonate liquid explosives (Subsect. IV-B). This suggests further examination of whether the experimental conditions or the chemical processes in these explosives can achieve hydrodynamic chemical equilibrium, and of whether their detonation products and reaction zones are single-phase fluids. To varying degrees, this might apply to other carbonate condensed explosives, as well as to very rich gaseous mixtures, e.g. [18–21]. The CJ-equilibrium model appears not to apply to carbonate condensed explosives, which supports a former conclusion by Davis, Craig and Ramsay, although for the opposite reason. Initial and detonation data for a non-carbonate liquid explosive would thus benefit further investigations. Ammonium nitrate NH_4NO_3 above its melting temperature (443 K) could be used, but its metastability at elevated temperatures raises a safety issue.

These features derive fairly easily from basic laws of hydrodynamics, namely the Rankine-Hugoniot relations contained in the single-phase adiabatic Euler equations. Their ubiquity today is the outcome of the prompting 40 years ago to develop numerical simulation of detonation dynamics. However, thermal and mechanical non-equilibria at elevated pressures and temperatures have long been a theoretical and numerical challenge. Averaged balance laws and constitutive relations built from various mixture rules are workarounds to fit in with this single-phase paradigm. The CJ supplemental properties can be used as go-betweens for experiments and models, in particular for coherently discussing this homogenization approach.

The hyperbolic Euler equations combined with explicit equations of state form a closed set for which a data distribution on a non-characteristic side of a discontinuity surface defines a well-posed Cauchy problem without using entropy. The sonic side of the CJ front is a particular case of characteristic distribution. Entropy was used here as an intermediate to obtain these new features without equation of state for the fluid on this characteristic side. The velocity of the surface and the initial state thus give the characteristic state, or the initial state and one characteristic-state variable give the velocity of the surface. This might be inherent to hyperbolic systems and the wider group of characteristic horizons, such as the surface of a Schwarzschild black hole. The CJ-equilibrium locus is the horizon of events in the TZD expansion for an observer in the ZND reaction zone.

Appendix A: Chapman-Jouguet relations for the perfect gas

The perfect gas is the ideal gas with constant heat capacities $\bar{C}_v = (R/W)/(\bar{\gamma} - 1)$ and $\bar{C}_p = (R/W)\bar{\gamma}/(\bar{\gamma} - 1)$, with W the molecular weight and $R = 8.31451$ J/mol.K the gas constant. The adiabatic exponent γ is the constant ratio $\bar{\gamma} = \bar{C}_p/\bar{C}_v$, the Gruneisen coefficient G is $\bar{\gamma} - 1$, the fundamental derivative Γ is $(\bar{\gamma} + 1)/2$, and an isentrope writes $pv^{\bar{\gamma}} = \text{const.}$ For the reactive perfect gas, the relation $T(p, v) = (W/R)pv$ reduces (3) to $dh(T) = C_p(T)dT$ whose integration gives the difference of enthalpies (A1) of the products at (T, p) and the fresh gas at (T_0, p_0) (neglecting the differences of their W and $\bar{\gamma}$), which substituted for $h - h_0$ in (14) then gives the Hugoniot (H) curve (A2):

$$h(p, v) - h_0(p_0, v_0) = \frac{\bar{\gamma}(pv - p_0v_0)}{\bar{\gamma} - 1} - Q_0, \quad (\text{A1})$$

$$p_H(v; v_0, p_0) = p_0 \times \frac{1 - \frac{\bar{\gamma}-1}{\bar{\gamma}+1} \left(\frac{v}{v_0} - \frac{2Q_0}{p_0v_0} \right)}{\frac{v}{v_0} - \frac{\bar{\gamma}-1}{\bar{\gamma}+1}}. \quad (\text{A2})$$

A CJ state is given by (27)–(29) with $\bar{\gamma}$ substituted for γ_{CJ} . A CJ velocity D_{CJ} is then a solution to the 2nd degree equation obtained by substituting v_{CJ} (27) and p_{CJ} (28) for p and v in (A2). The supersonic compressive solution (subscript CJc, Subsect. II-C) is the CJ-detonation velocity D_{CJc} ,

$$D_{\text{CJc}}(v_0, p_0) = \tilde{D}_{\text{CJ}} \left(\frac{1}{2} + \tilde{M}_{0\text{CJ}}^{-2} + \frac{1}{2} \sqrt{1 + 4\tilde{M}_{0\text{CJ}}^{-2}} \right)^{\frac{1}{2}}, \quad (\text{A3})$$

$$\tilde{D}_{\text{CJ}}^2 = 2(\bar{\gamma}^2 - 1)Q_0, \quad \tilde{M}_{0\text{CJ}} = \tilde{D}_{\text{CJ}}/c_0, \quad (\text{A4})$$

with dominant value \tilde{D}_{CJ} ($\tilde{M}_{0\text{CJ}}^{-2} \ll 1$) and acoustic (non-reactive) limit c_0 ($Q_0 = 0$). The subsonic expansive solution (subscript CJx) is the CJ-deflagration velocity D_{CJx} , deduced from D_{CJc} by changing the sign before the square root in (A3). They relate through

$$D_{\text{CJc}}D_{\text{CJx}} = c_0^2 \quad \text{or} \quad M_{0\text{CJc}}M_{0\text{CJx}} = 1, \quad (\text{A5})$$

which had not been pointed out before and shows that D_{CJx} has dominant value $\tilde{D}_{\text{CJ}}/\tilde{M}_{0\text{CJ}}^2 \equiv c_0/\tilde{M}_{0\text{CJ}}$. It can be used to express one solution with the other,

$$\frac{p_{\text{CJc}} - p_{\text{CJx}}}{p_{\text{CJc}}} = \dots$$

$$\dots \frac{1 - M_{0\text{CJc}}^{-4}}{1 + M_{0\text{CJc}}^{-2}/\bar{\gamma}} = 1 - \frac{M_{0\text{CJc}}^{-2}}{\bar{\gamma}} + \mathcal{O}\left(\frac{M_{0\text{CJc}}^{-2}}{\bar{\gamma}}\right)^2, \quad (\text{A6})$$

$$\frac{v_{\text{CJx}} - v_{\text{CJc}}}{v_{\text{CJx}}} = \dots$$

$$\dots \frac{1 - M_{0\text{CJc}}^{-4}}{1 + \bar{\gamma}M_{0\text{CJc}}^{-2}} = 1 - \bar{\gamma}M_{0\text{CJc}}^{-2} + \mathcal{O}(\bar{\gamma}M_{0\text{CJc}}^{-2})^2. \quad (\text{A7})$$

There are two overdriven detonation solutions ($Q_0 > 0$, $D \geq D_{\text{CJc}}$, Fig. 2). Only the upper (U) is a physical

intersect of a R line (13) and the H curve (A2) (subsonic, $M < 1$, Subsect. II-B). It writes

$$\frac{v}{v_0}(D, v_0, p_0) = \frac{\bar{\gamma} - \sqrt{\Delta_D} + M_0^{-2}}{\bar{\gamma} + 1}, \quad (\text{A8})$$

$$\frac{v_0 p}{D^2}(D, v_0, p_0) = \frac{1 + \sqrt{\Delta_D} + M_0^{-2}/\bar{\gamma}}{\bar{\gamma} + 1}, \quad (\text{A9})$$

$$\begin{aligned} \Delta_D &= \left(1 - \left(\frac{D_{\text{CJc}}}{D}\right)^2\right) \left(1 - \left(\frac{D_{\text{CJx}}}{D}\right)^2\right) \\ &= (1 - M_0^{-2})^2 - \left(\frac{\tilde{D}_{\text{CJ}}}{D}\right)^4. \end{aligned} \quad (\text{A10})$$

The lower (L) is non-physical (supersonic, $M > 1$). It is obtained by changing the sign before $\sqrt{\Delta_D}$ above. Both reduce to the shock solution (N) by setting $Q_0 = 0$, so $\sqrt{\Delta_D} = 1 - M_0^{-2}$ in (A8)-(A9). The theoretical CJ deflagration viewed as an adiabatic discontinuity with same initial state as the CJ detonation is not admissible (subsonic, $M_{0\text{CJx}} < 1$): (15) is not satisfied (Subsect. II-B, App. B). It was useful here for completeness and a simpler writing of relations (A8)-(A10) which reduce more obviously to the CJ relations (27)-(29) if $\Delta_D = 0$, that is, to v_{CJc} and p_{CJc} if $D = D_{\text{CJc}}$, or to v_{CJx} and p_{CJx} if $D = D_{\text{CJx}}$. From (A5), $(D_{\text{CJx}}/D)^2 = (c_0^2/DD_{\text{CJc}})^2 \leq M_{0\text{CJc}}^{-4} \ll 1$ that negligibly contributes to Δ_D compared to $(D_{\text{CJc}}/D)^2$: the typical values $c_0 = 300$ m/s and $D_{\text{CJc}} = 2000$ m/s give $D_{\text{CJx}} = 45$ m/s.

Appendix B: Chapman-Jouguet admissibility

The equilibrium expanding flow behind a CJ front is homentropic and self-similar (Subsect. III-A). The backward-facing Riemann invariant is thus uniform, that is, $du - (v/c)dp = 0$, and, since $u_p < u_{\text{CJ}}$, the material speed u (as well as p and v^{-1}) and the frontward-facing perturbation velocity $u + c = x/t$ have to decrease from the CJ front so expansion can spread out. Differentiating $u + c$ and expressing p and c as functions of s and v thus give $\Gamma^{-1}d(u + c) = du = vdp/c = -cdv/v$ [34], hence the constraint $\Gamma > 0$. Similarly, T decreases if $G > 0$ (6).

Using (22), the second-order differentials of $h(s, p)$, $p(s, v)$ and the Hugoniot relation give

$$\frac{F_{\text{CJ}}}{2} \frac{\partial^2 p_{\text{H}}}{\partial v^2} \Big|_{\text{CJ}} = \frac{\partial^2 p_{\text{S}}}{\partial v^2} \Big|_{\text{CJ}} = 2 \left(\frac{D_{\text{CJ}}}{v_0}\right)^3 \frac{\Gamma_{\text{CJ}}}{D_{\text{CJ}}}, \quad (\text{B1})$$

$$\frac{v_0^2 T_{\text{CJ}}}{D_{\text{CJ}}^2} \frac{\partial^2 s_{\text{R}}}{\partial v^2} \Big|_{\text{CJ}} = -2 \frac{\Gamma_{\text{CJ}}}{G_{\text{CJ}}}, \quad (\text{B2})$$

$$\frac{v_0^2 T_{\text{CJ}}}{D_{\text{CJ}}^2} \frac{\partial^2 s_{\text{H}}}{\partial v^2} \Big|_{\text{CJ}} = 2 \left(\frac{v_0}{v_{\text{CJ}}} - 1\right) \frac{\Gamma_{\text{CJ}}}{F_{\text{CJ}}}, \quad (\text{B3})$$

which show that $F_{\text{CJ}} \neq 0$ (Subsect. III-B) is also the condition for finite Hugoniot curvature and entropy variations at a CJ point for physical isentropes ($\Gamma \neq 0$,

Subsect. III-D). The curvatures of a Hugoniot and an isentrope have the same sign if $F_{\text{CJ}} > 0$, that is, if $G_{\text{CJ}} < 2/(v_0/v_{\text{CJ}} - 1)$, that of the Hugoniot being the larger if $0 < G_{\text{CJ}} < F_{\text{CJ}} < 2/(v_0/v_{\text{CJ}} - 1) < 2$, which is the case for most fluids.

Using (24) and (75), the derivative of M with respect to v along a Hugoniot at a CJ point is

$$\left(\frac{\partial M_{\text{H}}}{\partial v}\right)_{\text{CJ}} = \frac{\Gamma_{\text{CJ}}}{v_{\text{CJ}}}, \quad (\text{B4})$$

which shows, since $\Gamma_{\text{CJ}} > 0$, that $M < 1$ above, and $M > 1$ below, a CJ point, hence $F_{\text{CJ}} > 0$, $\partial^2 p_{\text{H}}/\partial v^2|_{\text{CJ}} > 0$ and $\partial^2 s_{\text{H}}/\partial v^2|_{\text{CJ}} > 0$ from (B1) and (B3). Also, comparing the slopes of a Rayleigh-Michelson line, a Hugoniot and an isentrope (16), (17), (18) about a CJ point with $\Gamma > 0$ indicates that $0 < F < 2$ if $G > 0$, and $F > 2$ if $G < 0$. Therefore, a CJ point is physically admissible only on a convex Hugoniot arc. Also, s increases and M decreases with decreasing v , so the physical branch of this arc is above the CJ point. Other derivations use concavity of entropy $s(e, v)$ or convexity of energy $e(s, v)$.

Appendix C: A model problem

Let the differentials of the functions $\beta(w, x)$ and $\sigma(w, x)$ of the two variables w and x satisfy

$$\varepsilon d\beta = adw + bdx, \quad (\text{C1})$$

$$d\sigma = qdw + rdx, \quad (\text{C2})$$

where ε , a , b , q , r are finite functions of β , w and x . These relations define the constraints

$$\varepsilon \left(\frac{\partial \beta}{\partial x}\right)_w = b, \quad (\text{C3})$$

$$\varepsilon \left(\frac{\partial \beta}{\partial x}\right)_\sigma = a \left(\frac{\partial w}{\partial x}\right)_\sigma + b, \quad (\text{C4})$$

$$0 = q \left(\frac{\partial w}{\partial x}\right)_\sigma + r. \quad (\text{C5})$$

The last, (C5), is the triple product rule, given that (C2) is a total differential, that is,

$$d\sigma = \left(\frac{\partial \sigma}{\partial w}\right)_x dw + \left(\frac{\partial \sigma}{\partial x}\right)_w dx \quad (\text{C6})$$

$$\Rightarrow \left(\frac{\partial \sigma}{\partial x}\right)_w = - \left(\frac{\partial \sigma}{\partial w}\right)_x \left(\frac{\partial w}{\partial x}\right)_\sigma \Leftrightarrow r = -q \left(\frac{\partial w}{\partial x}\right)_\sigma. \quad (\text{C7})$$

Therefore, if either $\partial w/\partial x|_\sigma$ or $\partial \sigma/\partial x|_w \equiv r$ is zero, so is the other if $\partial \sigma/\partial w|_x \equiv q$ is finite and non-zero.

In the limit $\varepsilon = 0$, (C3) shows that

$$b^{(\varepsilon=0)} = 0 \quad (\text{C8})$$

if $\partial \beta/\partial x|_w^{(\varepsilon=0)}$ is finite, then (C4) shows that

$$\left(\frac{\partial w}{\partial x}\right)_\sigma^{(\varepsilon=0)} = 0 \quad (\text{C9})$$

if $\partial\beta/\partial x)^{(\varepsilon=0)}_\sigma$ is finite and $a^{(\varepsilon=0)}$ is finite and $\neq 0$, then (C5) shows that

$$\left(\frac{\partial\sigma}{\partial x}\right)^{(\varepsilon=0)}_w \equiv r^{(\varepsilon=0)} = 0 \Leftrightarrow \left(\frac{\partial w}{\partial x}\right)^{(\varepsilon=0)}_\sigma = 0 \quad (\text{C10})$$

if $q^{(\varepsilon=0)} \equiv \partial\sigma/\partial w)^{(\varepsilon=0)}_x$ is finite and $\neq 0$. The constraints above and (C6) thus imply the equivalence $(d\sigma)^{(\varepsilon=0)} = 0 \Leftrightarrow (dw)^{(\varepsilon=0)} = 0$, but not that $(d\sigma)^{(\varepsilon=0)}$ or $(dw)^{(\varepsilon=0)}$ is zero. The DSI theorem (Subsect. III-C) is the application for which $\varepsilon = 1 - M$, $\sigma = s$, $\beta = v$, p or h , $w = D$,

$x = v_0$, $a \propto K_z \neq 0$, $q \propto K_s \neq 0$, $b \propto \Phi_z^*$ and $r \propto \Phi_s^*$.

If the arguments of $b(\beta, w, x)$ and $r(\beta, w, x)$ include the same grouping $\mu_0(\beta, w, x)$, and if conditions exist for which $(d\sigma)^{(\varepsilon=0)} = 0$ or $(dw)^{(\varepsilon=0)} = 0$, eliminating μ_0 between the constraint $b^{(\varepsilon=0)}(\beta, w, x, \mu_0) = 0$ and $r^{(\varepsilon=0)}(\beta, w, x, \mu_0) = 0$ defines a compatibility relation between β , w and x , that is, $\beta = \beta^{(\varepsilon=0)}(w, x)$, which then returns $\mu_0^{(\varepsilon=0)}$ by substituting $\beta^{(\varepsilon=0)}$ for β in either of these constraints. These are the operations in Subsection III-D that give v_{CJ}/v_0 and dp_0^*/dv_0 , here represented by μ_0 .

-
- [1] E. Jouguet, Sur la propagation des discontinuités dans les fluides, C. R. Acad. Sci. Paris **132**, 673 (1901).
 - [2] P. Vidal and R. Zitoun, A Velocity-Entropy Invariance theorem for the Chapman-Jouguet detonation (2020), arXiv:2006.12533 [physics.flu-dyn].
 - [3] H. Jones, The properties of gases at high pressures that can be deduced from explosion experiments, in *3rd Symp. on Combustion, Flame and Explosion Phenomena* (Williams and Wilkins, Baltimore, 1949) pp. 590–594.
 - [4] K. P. Stanyukovich, *Non-stationary flows in continuous media* (Pergamon Press, London (transl. State Publishers of Technical and Theoretical Literature, Moscow, 1955), 1960).
 - [5] N. Manson, Une nouvelle relation de la théorie hydrodynamique des ondes de détonation, C. R. Acad. Sci. Paris **246**, 2860 (1958).
 - [6] P. Vieille, Rôle des discontinuités dans la propagation des phénomènes explosifs, C. R. Acad. Sci. Paris **130**, 413 (1900).
 - [7] G. J. Sharpe, The structure of planar and curved detonation waves with reversible reactions, Phys. Fluids **12(11)**, 3007 (2000).
 - [8] A. Higgins, Steady one-dimensional detonation, in *Shock Waves Sciences and Technology Reference Library, Vol.6: Detonation dynamics* (Springer-Verlag, Berlin, Heidelberg, 2012) pp. 33–105.
 - [9] C. M. Tarver, On the existence of pathological detonation waves, in *13th APS Topical Conf. on Shock Compression of Condensed Matter* (2003).
 - [10] C. M. Tarver, Chemical energy release in several recently discovered detonation and deflagration flows, Journal of Energetic Materials **28:sup1**, 1 (2010).
 - [11] Y. B. Zel'dovich and A. S. Kompaneets, *Theory of detonation* (Academic Press, New York (transl. Gostekhizdat, Moscow, 1955), 1960).
 - [12] W. W. Wood and J. G. Kirkwood, Diameter effect in condensed explosives. the relation between velocity and radius of curvature of the detonation wave, J. Chem. Phys. **2(11)**, 1920 (1954).
 - [13] L. He and P. Clavin, On the direct initiation of gaseous detonations by an energy source, J. Fluid Mech. **277**, 227 (1994).
 - [14] A. R. Kasimov and D. S. Stewart, On the dynamics of self-sustained one-dimensional detonations: a numerical study in the shock-attached frame, Phys. Fluids **16(10)**, 3566 (2004).
 - [15] M. Short, S. J. Voelkel, and C. Chiquete, Steady detonation propagation in thin channels with strong confinement, J. Fluid Mech. **889**, A3 (2020).
 - [16] A. N. Dremin, *Towards detonation theory* (Springer, New York, 1999).
 - [17] C. M. Tarver, Condensed matter detonation: theory and practice, in *Shock Waves Sciences and Technology Reference Library, Vol.6: Detonation dynamics* (Springer-Verlag, Berlin, Heidelberg, 2012) pp. 339–372.
 - [18] G. B. Kistiakovski, H. T. Knight, and M. E. Malin, Gaseous detonations. IV. The acetylene-oxygen mixtures, J. Chem. Phys. **20**, 884 (1952).
 - [19] G. B. Kistiakovski and W. G. Zinman, Gaseous detonations. VII. A study of thermodynamic equilibrium in acetylene-oxygen waves, J. Chem. Phys. **23**, 1889 (1955).
 - [20] G. B. Kistiakovski and P. C. J. Mangelsdorf, Gaseous detonations. VIII. Two-stage detonations in acetylene-oxygen mixtures, J. Chem. Phys. **25**, 516 (1952).
 - [21] I. S. Batraev, A. A. Vasil'ev, V. Y. Ul'yanitskii, A. A. Shtertser, and D. K. Rybin, Investigation of gas detonation in over-rich mixtures of hydrocarbons with oxygen, Combustion, Explosion, and Shock Waves **54**, 207 (2018).
 - [22] J. Berger and J. Viard, *Physique des explosifs solides (p.186-190)* (Dunod, Paris, 1962).
 - [23] S. Bastea, Nanocarbon condensation in detonation, Nature Scientific Reports **7**, 42151 (2017).
 - [24] L. Edwards and M. Short, Modeling of the cellular structure of detonation in liquid explosives, in *abstract H05.008, APS Division of Fluid Dynamics* (2019).
 - [25] Y. N. Denisov and Y. K. Troshin, Pulsating and spinning detonation of gaseous detonation in tubes, Dokl. Akad. Nauk. SSSR **125**, 110 (1959).
 - [26] D. Desbordes and H.-N. Presles, Multi-scaled cellular detonation, in *Shock Waves Sciences and Technology Reference Library, Vol.6: Detonation dynamics* (Springer-Verlag, Berlin, Heidelberg, 2012) pp. 281–338.
 - [27] P. A. Urtiew and A. S. Kusubov, Wall traces of detonation in nitromethane-acetone mixtures, in *5th Symp. (Int.) Detonation* (ONR, 1970) pp. 105–114.
 - [28] P. A. Persson and G. Bjarnholt, A photographic technique for mapping failure waves and other instability phenomena in liquid explosives detonation, in *5th Symp. (Int.) Detonation* (ONR, 1970) pp. 115–118.
 - [29] C. M. Tarver and P. A. Urtiew, Theory and modeling of liquid explosive detonation, Journal of Energetic Materials **28(4)**, 299 (2010).
 - [30] W. Fickett and W. C. Davis, *Detonation: theory and*

- experiment* (Dover Publications, Inc., 2000).
- [31] P. Duhem, Sur la propagation des ondes de choc au sein des fluides, *Z. Phys. Chem.* **69**, 160 (1909).
 - [32] H. A. Bethe, *The theory of shock waves for an arbitrary equation of state, Report 545* (OSRD, 1942).
 - [33] H. Weyl, Shock waves in arbitrary fluids, *Comm. Pure Appl. Math.* **2**, 103 (1949).
 - [34] P. A. Thomson, A fundamental derivative in gasdynamics, *Phys. Fluids* **14**(9), 1843 (1971).
 - [35] S. P. D'yakov, On the stability of shock waves, *Zh. Eksp. Teor. Fiz.* **27**, 288 (1954).
 - [36] V. M. Kontorovich, Concerning the stability of shock waves, *JETP* **6**(6), 1179 (1957).
 - [37] J. W. Bates and D. C. Montgomery, The D'yakov-Kontorovich instability of shock waves in real gases, *Phys. Rev. Letters* **84**(6), 1180 (2000).
 - [38] L. Brun, *The spontaneous acoustic emission of the shock front in a perfect fluid: solving a riddle* (Ref. report CEA-R-6337, Tech. Rep. (CEA, 2013)).
 - [39] P. Clavin and G. Searby, *Combustion waves and fronts in flows: flames, shocks, detonations, ablation fronts and explosion of stars* (Cambridge University Press, 2016).
 - [40] L. Landau, *cit. in Landau L. & Lifchitz E., Fluid mechanics, Chapt. IX, §88* (Pergamon, Oxford (1958), 1944).
 - [41] P. D. Lax, Hyperbolic systems of conservation laws, II, *Comm. Pure and Appl. Math.* **10**, 537 (1957).
 - [42] G. R. Fowles, Subsonic-supersonic condition for shocks, *Phys. Fluids* **18**(7), 776 (1975).
 - [43] S. Gordon and B. McBride, *Computer program for calculation of complex chemical equilibrium compositions and applications, I. Analysis* (Ref. 1311), Tech. Rep. (NASA, 1994).
 - [44] G. I. Taylor, The dynamics of the combustion products behind plane and spherical detonation fronts in explosives, *Proc. Roy. Soc. A* **200**, 235 (1950 (1941)).
 - [45] W. Döring and G. Burkhardt, *Beiträge zur Theorie der Detonation* (Ref. Bericht n° 1939), Tech. Rep. (Deutsche Luftfahrtforschung, 1944).
 - [46] W. W. Wood and W. Fickett, Investigation of the CJ hypothesis by the "Inverse Method", *Phys. Fluids* **6**(5), 648 (1963).
 - [47] W. C. Davis, Equation of state from detonation velocity measurements, *Comb. and Flame* **41**, 171 (1981).
 - [48] N. Manson, Semi-empirical determination of gas characteristics in the Chapman-Jouguet state, *Comb. and Flame* **2**(2), 226 (1958).
 - [49] F. Wecken, *Note Technique n° 459 (avril)*, Tech. Rep. (Institut Franco-Allemand de Saint-Louis, 1959).
 - [50] K. Nagayama and S. Kubota, Approximate method for predicting the Chapman-Jouguet state of condensed explosives, *Propellants, Explosives, Pyrotechnics* **29**(2), 118 (2004).
 - [51] S. A. Sheffield, L. L. Davis, R. Engelke, R. R. Alcon, M. R. Baer, and A. M. Renlund, Hugoniot and shock initiation studies of isopropyl nitrate, in *12th APS Topical Conf. on Shock Compression of Condensed Matter* (2001).
 - [52] F. Zhang, S. B. Murray, A. Yoshinaka, and A. Higgins, Shock initiation and detonability of isopropyl nitrate, in *12th Symp. (Int.) Detonation, San Diego, CA* (ONR, 2002) pp. 781–790.
 - [53] C. Brochet and F. Fisson, Détermination de la pression de détonation dans un explosif condensé homogène, Explosifs n° 4, pp. 113-120 (1969), and Monopropellant detonation: isopropyl nitrate, *Astronaut. Acta* **15**, 419 (1970).
 - [54] W. C. Davis, B. G. Craig, and J. B. Ramsay, Failure of the Chapman-Jouguet theory for liquid and solid explosives, *Phys. Fluids* **8**(12), 2169 (1965).
 - [55] P. C. Lysne and D. R. Hardesty, Fundamental equation of state of liquid nitromethane to 100 kbar, *J. Chem. Phys.* **59**(12), 6512 (1973).
 - [56] W. M. Jones and W. F. Giauque, The entropy of nitromethane. Heat capacity of solid and liquid. Vapor pressure, heats of fusion and vaporization, *J. Am. Chem. Soc.* **69**(5), 983 (1947).
 - [57] H. A. Berman and E. D. West, Density and vapor pressure of nitromethane 26° to 200°C., *J. Chem. and Eng. Data* **12**(2), 197 (1967).
 - [58] Y. Bernard, J. Brossard, P. Claude, and N. Manson, Caractéristiques des détonations dans les mélanges liquides de nitropropane II avec l'acide nitrique, *C. R. Acad. Sci. Paris* **263**, 1097 (1966).
 - [59] W. B. Garn, Detonation pressure of liquid TNT, *J. Chem. Phys.* **32**(3), 653 (1960).
 - [60] W. B. Garn, Determination of the unreacted Hugoniot for liquid TNT, *J. Chem. Phys.* **30**(3), 819 (1959).
 - [61] F. J. Petrone, Validity of the classical detonation wave structure for condensed explosives, *Phys. Fluids* **11**(7), 1473 (1968).
 - [62] M. Chiquete and M. Short, Characteristic path analysis of confinement influence on steady two-dimensional detonation propagation, *J. Fluid Mech.* **863**, 789 (2019).
 - [63] M. C. Branch, M. E. Sadequ, A. A. Alfarayedhi, and P. J. Van Tiggelen, Measurements of the structure of laminar, premixed flames of $CH_4/NO_2/O_2$ and $CH_2O/NO_2/O_2$ mixtures, *Combustion and Flame* **83**, 228 (1991).
 - [64] H. Presles, D. Desbordes, M. Guirard, and C. Gueraud, Gaseous nitromethane and nitromethane-oxygen mixtures: a new detonation structure, *Shock Wave* **6**, 111–114 (1996).
 - [65] L. E. Fried and P. C. Souers, BKWC: An empirical BKW parametrization based on cylinder test data, *Propellants, Explosives, Pyrotechnics* **21**, 215 (1996).
 - [66] M. Cowperthwaite and W. H. Zwisler, The JCZ equation of state for detonation products and their incorporation into the Tiger code, in *6th Symp. (Int.) on Detonation* (ONR, 1976) pp. 162–172.